

SIMULATION AND OPTIMIZATION OF A CONSTRUCTED WETLAND FOR BIOMASS
PRODUCTION AND NITRATE REMOVAL

BY

ARAS J. ZYGAS

THESIS

Submitted in partial fulfillment of the requirements
for the degree of Master of Science in Environmental Engineering in Civil Engineering
in the Graduate College of the
University of Illinois at Urbana-Champaign, 2010

Urbana, Illinois

Advisers:

Professor Ximing Cai
Professor Wayland Eheart

ABSTRACT

Recently there is growing concern about high nutrient loadings in surface waters as a result of intensive agriculture, resulting in hypoxia in coastal ecosystems. There is simultaneous growing interest in the cultivation of perennial grasses for bio-ethanol production. Constructed wetlands offer a promising nutrient removal mechanism while also providing an ideal environment for the growth of such grasses. In the present work, a hypothetical wetland system is designed to treat non-point source nutrient loadings and produce harvestable biomass for ethanol production in central Illinois. Through the integration of a biomass production model, a nutrient removal model and a cost model, the relationship between the costs of wetland construction, benefits from biomass sales, and mass nutrient removal can be seen for various wetland sizes and water throughput capacities. Using genetic algorithms, the Pareto-optimal frontier showing the tradeoff between nutrient removal and the net cost of the wetland system, (accounting for revenue from biomass harvest) can be visualized.

This analysis is demonstrated for a hypothetical wetland site near Camargo, Illinois which is assumed to draw water from the Embarras River. Through the simulation of several cost scenarios, the wetland is found to show a profit only when construction, operation and maintenance costs are excluded from the analysis. Results show a tradeoff between the amount of nitrate removed in the wetland via denitrification and biomass production. For the example case, a 33.8 ha wetland with a $2.3 \text{ m}^3/\text{s}$ design pumping capacity was found to have the maximum cost efficiency with a cost of 4.8 \$/kg of $\text{NO}_3\text{-N}$ removed. The results indicate that there is a unique efficiency-maximizing design for a wetland at a particular site. These results also indicate that a subsidy of at least 4.8 \$/kg of $\text{NO}_3\text{-N}$ removed is necessary (assuming the biomass is sold for \$58/ton) in order for a wetland at the hypothetical site to break even. Furthermore, if a market for nitrogen exists or if nutrient trading between point dischargers is allowed, it might be possible for a constructed wetland designed for biomass production to be profitable while providing water quality benefits.

ACKNOWLEDGEMENTS

Many thanks to my co-advisers Wayland Eheart and Ximing Cai for their unwavering support, key insights, and patience. I would like to thank Tze Ling Ng for her invaluable help with the technical portions of the project. Furthermore, thank you to Dr. Takashi Asaeda and Baniya Mahendra of Saitama University for assisting with the formulation of the biomass production model. Finally, thanks to my family and friends who were by my side during the entire process, offering unconditional encouragement.

TABLE OF CONTENTS

1. Introduction.....	1
1.1. Background.....	1
1.2. Objectives	7
2. Method	8
2.1. Biomass production model	8
2.2. Nutrient removal model	10
2.3. Biomass production and nutrient removal model considerations and interactions	15
2.4. Cost model	16
2.5. Genetic algorithm optimization	21
3. Results.....	24
3.1. Baseline scenario enumeration results	24
3.2. Baseline scenario genetic algorithm results	30
3.3. Baseline scenario cost-per-removal results.....	34
4. Discussion.....	36
5. Conclusions and Recommendations	43
6. References.....	46

1. Introduction

This thesis analyzes the economic efficiency of a constructed wetland for both nutrient removal and biomass harvest in the Midwestern United States. Extensive crop fertilization in the region has led to nutrient-based water quality issues, the effects of which can be seen not only in inland water bodies, but also as far as the Gulf of Mexico. One method of mitigating such pollution that has been gaining recent attention is the constructed wetland, a series of one or more shallow pools planted with aquatic vegetation that is engineered for the purpose of improving water quality. Unfortunately the large capital cost associated with the construction of wetlands has led them to be an uncommon option for the treatment of non-point source pollution. However, the agricultural landscape of the Midwest could undergo drastic changes due to technological advancements in ethanol production that have been promoted by the national mandate of biofuel production. Such advancements may provide a new opportunity for constructed wetlands since the perennial grasses currently being considered for biofuel feedstocks in the Midwest share many of the same admirable characteristics as the vegetation found in natural wetlands. The highly productive, highly tolerant, low input perennial grasses provide an attractive alternative to the relatively inefficient process of producing fuel from corn and soybeans, and not displacing the supply of those grains for other uses (primarily food). This leads to the hypothesis of the study: Through the cultivation of wetland vegetation in a constructed wetland benefits can be realized in the form of water quality treatment as well as monetary revenue from the sale of biomass to ethanol processing facilities. In order to determine the feasibility of such a system, a hypothetical wetland in central Illinois will be simulated and its design will be optimized to assess relationships between wetland design parameters and the tradeoff between system cost and nutrient removal with consideration of biomass harvest profit.

1.1. Background

Being one of the most intensely cultivated and fertilized states in America, Illinois is prone to nutrient-based water quality issues. One of the most problematic of such pollutants is nitrogen, which arises primarily from the fertilization of corn. The primary crops grown in Illinois are corn and soybeans, which account for 60% of the total land area of the state as estimated by the National Agricultural Statistics Service. As the excess fertilizer runs off the fields, it ends up in streams and lakes and eventually contributes to drinking water problems, eutrophication, as well as hypoxia in coastal waters. The poorly drained soils of Illinois have led to an agricultural landscape dominated by tile drainage, which expedites the transport of nutrients from the field to the stream. To counter this effect partially, many best

management practices (BMPs) have been adopted to help with nutrient runoff control. As opposed to point sources, non-point source pollution is much more difficult to control and treat. By enrolling in a nutrient management plan, practicing conservation tillage, planting filter strips, or adopting various other BMPs, farmers may earn compensation from the local or state government, while doing their part to help control nutrient runoff. These best management practices generally require a change in operations (such as specialized equipment for conservation tillage or different fertilizer application levels, times, and depths) or a small land commitment (planting grass filter strips along drainage ditches). According to the Lake Bloomington Watershed TMDL Implementation Plan (2008), farm-level BMPs vary greatly in their ability to remove nitrogen. For example, filter strips have been shown to reduce nitrogen anywhere from 27% to 87% (Lake Bloomington TMDL, 2008). It is the spatial variability of nutrient loads and abatement efficiencies of BMPs that causes this range of nutrient removal efficiencies. Nevertheless, compared to point-source treatment, BMPs offer an opportunity to improve water quality relatively inexpensively that should not be ignored. According to the Lake Bloomington Watershed TMDL Implementation Plan, the cost of farm-level BMPs ranges from \$1/ac/yr (for a nutrient management plan) to \$27.50/ac/yr (for a filter strip).

One method for nutrient abatement that has received recent attention is the constructed wetland, i.e., a series of one or more shallow pools planted with aquatic vegetation that is engineered to improve water quality. Constructed wetlands are designed to mimic the physical, chemical and biological processes that occur in natural wetlands in order to reproduce the water quality benefits that natural wetlands provide. Along with water quality benefits, wetlands (constructed or natural) have the potential to provide recreational services as well as wildlife restoration. As opposed to the BMPs mentioned above, constructed wetlands require a relatively large land area and nontrivial capital investment. Through an empirical study, Kovacic et al. (2006) determined that if 5% of the Lake Bloomington Watershed (1,112 acres) was converted to constructed wetlands at a cost of \$1,500/acre/year (assuming a 50-year operational lifetime and neglecting the cost of land), nitrogen loadings at the watershed outlet would be reduced by 46%. Other studies have also indicated that wetlands make significant improvements in water quality. According to a survey of 17 sites in North America and Northern Europe done by Braskerud et al. (2005), constructed wetlands were capable of up to an 89% removal rate for nitrogen. In Illinois, a 37% reduction in total nitrogen was estimated by Kovacic et al. (2000) at three sites treating tile drainage water; while a mass percent removal of 39-99% of nitrate was reported by Hey et al. (1994) treating stream water from the Des Plaines River. While government incentives exist to help with the costs of restoring natural wetlands, the financial burden and land commitment of creating constructed wetlands precludes them from being commonplace. As the biofuel industry continues to make advances in

producing ethanol from cellulosic biomass, there may be a way for wetlands to become less expensive or even profitable by providing both biomass and nutrient removal services.

Currently in the Midwest, biofuel crops consist of corn and soybeans from which the sugar, starch and oils are converted to ethanol or biodiesel through fermentation or transesterification. The problem with using corn and soy for biofuels is that these crops are already used for food. Moreover, inefficient conversion technologies and unfavorable energy balances make corn and soy a poor choice for biofuel production. The emerging political climate for biofuels is currently shifting away from processing sugars, starch and oils to methods involving converting cellulose to ethanol. Cellulosic ethanol is promising since conversion technologies allow for the use of all types of lignocellulosic biomass. Anything from perennial grasses to wood to crop residues can be used as a feedstock, thus eliminating competition with food. The goal is to find a crop that requires few inputs, grows quickly and/or on land not currently used for conventional row crops, produces a large yield, can be processed efficiently and is sustainable (Sims et al., 2006). Current studies are examining the feasibility of growing perennial grasses such as switchgrass (*Panicum virgatum*) and miscanthus (*Miscanthus x giganteus*) in Illinois as biofuel feedstocks (e.g., Khanna et al., 2008). Switchgrass and miscanthus require few inputs, can have high yields even on marginal (i.e. flood-prone) land, and have the potential to provide environmental benefits such as carbon sequestration. Plants with similar lignocellulosic content to switchgrass and miscanthus have adapted to growing in wetlands and are highly productive. The highly productive nature of wetland emergent macrophytes makes them a possible feedstock in producing cellulosic ethanol, with the added benefit of water quality improvement. This research holds out the promise of being able to use constructed wetlands as a means of sustainable agriculture while providing quantifiable water quality improvement.

The purpose of this research is to develop and apply a mathematical model to simulate and optimize a hypothetical constructed wetland specially designed for the dual purpose of water quality improvement (specifically conversion of nitrate to elemental nitrogen) and biomass production. Through the coupling of a wetland denitrification model, a plant biomass simulation model, and an economic model it is possible to obtain the biomass yield, nutrient reduction and cost of a hypothetical wetland for biomass production. Using genetic algorithms, a cost-optimal size (area) and pumping rate (wetland throughput) are determined for a constructed wetland for biomass harvesting and nutrient removal. The theoretical wetland receives water from the Embarras River near Camargo, Illinois. The water is then fed through the wetland and returned to the river. The Embarras watershed is chosen because it is intensively cultivated and therefore represents a typical agricultural watershed in Illinois. Furthermore, nitrogen data from the Embarras River are readily available.

Emergent aquatic plants have a history of being harvested for various uses. *Papyrus* in Egypt, *Schoenoplectus* in Bolivia and *Phragmites* in Europe and the Middle East have been harvested for use as building material for houses (thatched roofs) and rafts as well as fuel (for burning). Reed is also used as a raw material in cellulose production, which began after World War II on the Danube delta. Since many lakes have been drained in Sweden to provide more arable land (as has occurred in the Midwest), many of the nation's wetlands were lost. Along with the loss of wetlands, the oil crisis of 1973-74 sparked some of the first investigations of the use of wetland plants as an energy source. In Sweden, the Swedish National Board for Energy Source Development began funding research on the use of reeds (*Phragmites australis*) for energy. The motivation was that if an economic gain could be had from harvesting wetlands for reed biomass, this would help conserve or even expand the threatened wetland areas. Granéli (1984) examined the problems and solutions in regard to using reed as an energy source in Sweden. The studies performed by Granéli (1984), however, referred to the harvest of *natural* wetland biomass as opposed to biomass cultivated in a *constructed* wetland. Complications arise for natural wetlands since conditions are extremely variable and in most cases harvesting must be done in saturated conditions or on ice. Being able to control the water-depth of constructed wetlands makes the harvesting procedure much simpler.

Granéli's analysis focused mainly on the profitability of harvesting reed as a fuel for burning with the hope of wetland restoration as an ancillary benefit. With recent attention to non-point source water quality problems such as hypoxia in the Gulf of Mexico as well as technological developments that may make plants such as *Phragmites* viable as a biofuel feedstock, constructed wetlands may offer an opportunity to curb dependence on fossil fuels while also providing water quality benefits. While there are a multitude of studies that address the efficiency and applicability of constructed wetland systems in terms of water quality improvement, few focus on biomass harvesting. Toet et al. (2005) conducted a study on two emergent wetland plant species receiving effluent from a sewage treatment plant to determine if autumn harvest would be a sufficient means of nutrient removal. The mean NO₃-N concentrations received by the stands were 1.54 mg/L in the first year, and 3.26 mg/L in the second year and the hydraulic residence time (HRT) was varied between 0.8 and 9.3 days. The findings suggest that harvesting biomass for nutrient removal becomes less efficient as the nutrient mass input increases since plants only take up a small fraction of passing nutrients (denitrification was found to be the major pathway of N removal in the constructed wetlands). As is the case with most constructed wetlands, the wetlands in the study by Toet et al. (2005) are designed to treat relatively low and consistent nutrient concentrations coming from a wastewater treatment plant. While natural wetlands provide water quality benefits for non-point source loadings, quantifying nutrient removal becomes an issue due to uncertainty about the various sources and

pathways that water and nutrients take in their journey from the crop field through the wetland. In this study, by assuming that the hypothetical constructed wetland is lined and receives flow directly from the Embarras River, the seasonal variation in both flow and nutrient concentrations can be quantified while minimizing the effect of other water fluxes (infiltration, runoff, etc.) on the analysis.

The choice of vegetation (i.e. crop) is extremely important in the design of a constructed wetland. Wetland plants influence oxygen levels in the wetland water and soil and help provide underwater surface area for the colonization of denitrifying bacteria. If a treatment wetland is also to be harvested, the chosen vegetation should also produce sufficient amounts of harvestable biomass. The hypothetical wetland will be planted with *Phragmites australis* (common reed). *Phragmites* was chosen because it is fast-growing, highly productive, perennial, and quite tolerant of extreme conditions. Moreover, data exist about the growth habits and patterns of *Phragmites* (Hosoi et al., 1998; Allirand & Gosse, 1995; Meuleman et al., 2002; Haslam, 1969b; Engloner, 2009). It is important to note, that although *Phragmites* has admirable characteristics for a wetland plant to be harvested for biomass, the uncontrolled propagation of *Phragmites* has led it to become regarded as an invasive species in 18 states (Getsinger, 2007). Although *Phragmites* is currently not considered invasive in Illinois, the fact that the plant is considered noxious in the neighboring states of Wisconsin, Indiana, Kentucky, Ohio and Michigan suggest that unmonitored stands could pose a threat to native species in Illinois as well.

As mentioned above, *Phragmites* has actually been considered as a biofuel crop in Sweden during the oil crisis in the 1970s (Granéli, 1984). While *Phragmites australis* (Cav.) Trin. ex Steudel can be found worldwide, the distribution and abundance has radically increased in the United States in the past 100 years. *Phragmites* is present in North America in both native and non-native forms. Haplotypes E and S of the plant are indigenous to North America while haplotype M plants are native to Europe and Asia. While the physical differences between haplotypes is difficult to detect by observation, evidence shows that the non-native haplotype M is rapidly replacing indigenous reed populations (Saltonstall, 2002). The formation of large monospecific stands of *Phragmites* threatens native wetland species such as *Typha* spp. and *Spartina* spp. (Ailstock et al., 2001).

However, the plant's potential usefulness for environmental enhancement has led to differences in opinion on the ecological value of *Phragmites*. Research has shown that the common reed can be an important soil stabilizer and has applications as a nutrient sink for treating wastewater (Bonham 1983; Kamio 1985; Gersberg et al. 1986; Brix 1987; House et al. 1994). Moreover, perennial grasses such as miscanthus that are being considered for biofuel feedstocks in Illinois may pose invasion issues if their

cultivation becomes widespread. Regardless of what type of crop is chosen, there will be foreseen and unforeseen environmental impacts. The essential question is whether the environmental benefits of growing a biofuel feedstock outweigh the negative environmental impacts (Ditomaso et al., 2010). *Phragmites* has been one of the most frequently chosen plants for constructed free water surface wetlands throughout the United States (NADB v.2). It is worth noting that the NADB v.2 database only contains an early subset of free water surface systems and recently constructed systems are not included.

The purpose of this research is not to promote the planting of an invasive species as a biofuel crop, but to simulate how emergent wetland plants could potentially be used as a biofuel feedstock. Other, native Illinois plants such as *spartina pectinata* (prairie cordgrass) may have potential for a dual purpose wetland, but severe data limitations restrict any type of biomass growth simulations. The results of this research should be viewed as a feasibility study for the use of wetlands for hydrophilic biomass production and nitrate treatment in general, not one focused on *Phragmites* in particular.

Besides the revenue from biomass sales, constructed wetlands have the potential to earn capital in other ways as well. Hey (2002) investigates the possibility of reducing nitrate-nitrogen concentrations in the Illinois River through the combination of wetland restoration (nitrogen farms) and a nitrogen market. He estimates that the restoration of 162,000 ha of wetlands in the Illinois River watershed would reduce the total loading of $\text{NO}_3\text{-N}$ to the Gulf of Mexico by 10% and cost half as much as using a conventional treatment method (involving concrete tanks, pumps and electrical and chemical energy). Apart from the potential benefits associated with nutrient credit trading, government incentives or subsidies could play a role in making constructed wetlands profitable. Currently, the Wetland Reserve Program (WRP) offers financial compensation to landowners who protect, restore and enhance wetlands on their property. While the current focus of the WRP is to restore natural wetlands, it could be foreseeable that in the future constructed wetlands might be eligible for compensation, assuming that such wetlands could provide the same water quality and wildlife habitat benefits. Although constructing a wetland is more costly than restoring a natural wetland, the possibility to control the system (i.e. the flow through the wetland) has advantages in both the nutrient removal potential of the wetland, and the ease of monitoring. Moreover, compared to other methods of non-point source nitrate-nitrogen abatement (e.g. conventional treatment technologies, BMPs employment) wetlands are hailed as one of the most cost efficient options (whether they are constructed or natural) (Kadlec, 2009).

While previous studies focus on the harvesting of emergent aquatic vegetation from natural wetlands or the efficiency of constructed wetlands when treating sewage treatment effluent, this study offers a unique analysis of the use of a constructed wetland for the treatment of non-point source nitrate-nitrogen loadings while simultaneously providing a controlled environment for the growth and harvest of emergent macrophytes for sale as a biofuel feedstock.

1.2. Objectives

The goal of this study is to assess the economic feasibility of using a constructed wetland for both biomass production and nitrate removal by simulating a hypothetical wetland located near Camargo, Illinois receiving effluent from the Embarras River. The specific objectives are as follows:

1. Simulate a hypothetical wetland that adequately portrays biomass production and nutrient dynamics.
2. Assess the costs and benefits of using such a constructed wetland for biomass production and nitrogen reduction.
3. Use genetic algorithms to find the optimal wetland area and pumping capacity and the non-inferior set between cost and nutrient removal.
4. Explore various scenarios of biomass price and nutrient removal requirements and associated tradeoffs.

2. Method

Simulation of a hypothetical wetland for biomass production requires the integration of three separate models; a biomass production model, a nutrient removal model and a cost model. The biomass production model simulates biomass yields, the nutrient removal model simulates denitrification in the wetland and the economic model estimates the costs and benefits of constructing and operating the wetland. Figure 2.1 shows a diagram outlining how the three models are combined. The three integrated models are then optimized using genetic algorithms to find the Pareto front of the two decision variables (pumping capacity and wetland area) for the two objectives, viz., cost and nutrient removal.

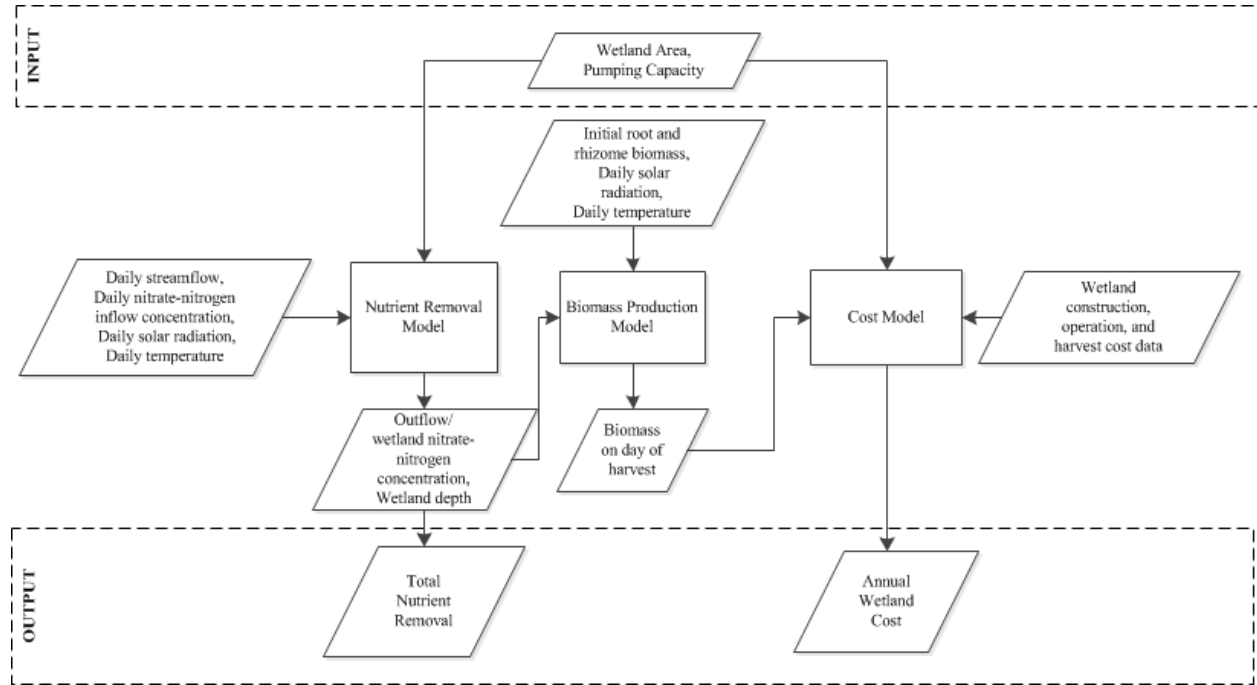


Figure 2.1: Simulation model schematic diagram

2.1. Biomass production model

Due to the importance of the *Phragmites* to the environment and as a commodity, stand phenology and biomass production has been studied extensively in the field (Haslam, 1969b, 1970; Hocking, 1989a,b). Although characteristics such as leaf area production, energy absorption, and conversion efficiencies have been evaluated in different locations (Dykyjova and Pribil, 1975; Ho, 1979; Hocking, 1989a; Hara et al., 1993; Allirand and Gosse, 1995), these studies depended on empirical relationships thus limiting the scope of understanding the growth dynamics of the common reed. The fact that the mean caloric values of

vascular aquatic plants do not vary much (Boyd, 1970; Kaul and Vass, 1972) allowed for the successful simulation of the growth of various plants through the use of mathematical modeling (Scheffer et al., 1993; Asaeda and Bon, 1997). A growth dynamics simulation model developed by Asaeda and Karunaratne (2000) is used to simulate biomass production for the hypothetical wetland. The model was constructed in a highly mechanistic fashion focusing more on the internal physiological mechanisms of biomass production in the plant rather than relying heavily on empirical data-driven relationships to describe the growth of the plant. Due to the lack of empirical *Phragmites* data in the Midwest, a more mechanistic growth model proves to be preferable. The model is applicable to well-established, monospecific stands of *Phragmites australis* in shallow lakes, ponds, freshwater swamps and their margins.

Using first order differential equations in a plant-phenology framework, the biomass production model simulates the live growth characteristics of *Phragmites*. The five state variables used to illustrate plant growth are the biomass per square meter of shoots, inflorescence, roots, old rhizomes and new rhizomes. New rhizomes are defined as those formed during the current growing season. The combined effect of photosynthesis, respiration, mortality, and translocation of photosynthesized material between shoots and below-ground plant organs describes the net production of the stand. Five growth equations (one for each plant organ) were developed, tracking the aforementioned processes. Subdivision of the above-ground biomass into stratified 1-cm thick horizontal layers was used to calculate separately the dry matter budget and elongation. The growth equations were solved simultaneously for each layer using the Fourth order Runge-Kutta method with a daily time step (Cheney, 2004). The input data for the model are the rhizome and root biomass (g/m^2) before the emergence of shoots, the daily total surface irradiance ($\mu\text{mol/m}^2/\text{day}$) and the daily mean air temperature ($^{\circ}\text{C}$). The daily irradiance and temperature data for Champaign, Illinois were obtained from the Illinois State Water Survey's Water and Atmospheric Resources Monitoring Program (WARM) database. The initial root and rhizome biomass values were taken from observed data from Lake Kasumigaura in central Japan provided by Sakurai et al. (1985). Since the data from Sakurai et al. (1985) come from a region that is similar in latitude and climate to the hypothetical wetland site, it is assumed that the initial below-ground biomass at the Japanese site provides an adequate approximation to the initial conditions that would be experienced in Illinois.

All mathematical models require parameter evaluation, which can be done by many different methods. The unknown parameters used in the model were calibrated using four experimental data sets (the same parameters were used for each simulation). Observed data from studies by Hocking (1989a, b), Kvet et al. (1969) and Sakurai et al. (1985) in Australia (two studies), the Czech Republic, and Japan, respectively

were used in the model calibration. The use of data from various locations and various natural conditions ensures that the model can be used over a wide range of climatic conditions.

The approximate dates of phenological events (i.e. different phases in the plant's lifecycle) are of great importance when formulating the model. Experimental data and regression analysis were used to form simple mathematical relationships in order to describe the plant phenology. For example, while the panicle emergence time varies with climatic region, a comparison of the period of panicle emergence and maximum day length shows that the two events are closely related. Therefore, if the maximum day length is known, the date of panicle appearance can be calculated. Physical factors (soil and air temperature, water regime, frosts, biotype, etc.) and biological factors (nature and status of rhizome reserves, etc.) that affect the phenological cycle were not explicitly accounted for in the simulation model. Furthermore, it is assumed that the reed stand undergoes a one-batch phenological cycle while in reality different portions of the stand go through different phenological cycles at slightly different times.

The output variables of the model are the biomass of the five plant organs for a given growing season. The model was used to determine the annual total biomass yield and assess the relationship between yield and the decision variables (wetland area and pumping capacity).

2.2. Nutrient removal model

For the nutrient removal model, time steps of 0.5, 1, and 2 days were compared to determine whether a one-day time step would suffice for the model simulation. Since only daily data were available, the nutrient removal model with a half-day time step was run using linear interpolation of the daily input data. The negligible differences in the outflow $\text{NO}_3\text{-N}$ concentration between the three different time steps suggest that a time step of one day is sufficiently small to provide accurate results for the nutrient removal model.

One of the major differences between the nutrient removal and biomass production models is the method used to solve the differential equations involved. A backward difference (Euler) scheme is used in the nutrient removal model while the Runge-Kutta method is utilized in the biomass production model. Although the biomass production model might have utilized an Euler scheme adequately, the nonlinear growth model implied a need for a higher level of accuracy, which led to the use of the Runge-Kutta method in the biomass production model formulation by Asaeda and Karunaratne (2000). Furthermore, as a test of accuracy, the timestep of the nutrient removal model was altered from 1 to 0.5 days, which did

not show a noticeable difference in output and which obviates the need for the higher accuracy provided by the Runge-Kutta method.

The nutrient removal model used in this analysis assumes first order denitrification kinetics under perfectly mixed conditions. While water pumped directly from the Embarras River is the primary inflow (source) in the wetland system, there are other water sources or sinks that may be important. The overall water mass balance for a wetland is:

$$q - Q_o + Q_c - Q_b - Q_{gw} + Q_{sm} + (P \times A) - (ET_c \times A) = \frac{dV}{dt} \quad (2.1)$$

where

A = wetland surface area, m²
 ET_c = evapotranspiration rate, m/d
 P = precipitation rate, m/d
 Q_b = bank loss rate, m³/d
 Q_c = catchment runoff rate, m³/d
 Q_{gw} = net infiltration to groundwater, m³/d
 q = input flowrate, m³/d
 Q_o = output flowrate, m³/d
 Q_{sm} = snowmelt rate, m³/d
 t = time, d
 V = water storage (volume) in wetland, m³

Beyond the input and output flows, rainfall and evapotranspiration are usually the most significant. Depending on the location, groundwater infiltration and bank loss may also prove significant. However, in the case studied here, bank losses and infiltration can be neglected since it is assumed that the hypothetical wetland will be constructed with a liner. The daily mass balance used in the wetland nutrient removal simulation then becomes:

$$q - Q_o + (P \times A) - (ET_c \times A) = \frac{dV}{dt} \quad (2.2)$$

In order to calculate the evapotranspiration, the $K_c ET_0$ approach is used. This approach takes into account the effect of climate on crop water requirements through a reference-crop evapotranspiration ET_0 while the effect of the crop is characterized by the crop coefficient K_c . The reference crop evapotranspiration rate is estimated using the Hargreaves (Hargreaves et al., 1985) equation:

$$ET_0 = 0.0135RS \times (T_C + 18) \quad (2.3)$$

where

ET_0 = reference crop evapotranspiration with Alta fescue grass as the reference crop

RS = solar radiation at the surface in equivalent water evaporation

T_C = mean temperature, °C

Surface radiation, temperature and precipitation data from the Illinois State Water Survey's Water and Atmospheric Resources Monitoring Program (WARM) database for Champaign, Illinois were used in the simulation. Equivalent evaporation in m/day can be calculated from radiation expressed in MJ/m²/day by a conversion factor equal to the inverse of the latent heat of vaporization.

$$RS[\text{m/day}] = \frac{RS[\text{MJ/m}^2/\text{day}]}{\lambda\rho} \quad (2.4)$$

where λ is the latent heat of vaporization (2.45 MJ/kg) and ρ is the density of water (1000 kg/m³). Once ET_0 is calculated, the crop evaporation under standard conditions (ET_C) can be calculated by the following relation:

$$ET_C = K_C ET_0 \quad (2.5)$$

The dimensionless crop coefficient K_C integrates the effect of characteristics that distinguish certain plants from the grass reference. For *Phragmites*, a K_C value of 1.2 is chosen, which corresponds to values empirically obtained for a 'reed swamp in standing water' by the Food and Agriculture Organization of the United Nations (Allen et al., 1998).

If it is assumed that the nitrate concentration in precipitation is negligible, the nutrient mass balance of the wetland can be represented as:

$$\frac{d(CV)}{dt} = Bq - CQ_o - kAC \quad (2.6)$$

where C = wetland outflow nitrate concentration (assumed to be the same as within the wetland), B = wetland inflow nitrate concentration, q = wetland inflow and k = first order areal decay coefficient. The temperature dependent rate coefficient k is found using the following relationship:

$$k = K(\tau)^{T_c - 20} \quad (2.7)$$

where K is the first-order areal decay coefficient at 20°C and τ is the temperature correction factor. For nitrate $K = 35$ m/yr and $\tau = 1.09$ (Kadlec and Knight, 1995). Discretizing equation (2.6) using a backward difference scheme gives, for time step n :

$$C_n = \frac{B_n q_n \Delta t + C_{n-1} V_{n-1}}{V_n + Q_{0n} \Delta t + k_n A \Delta t} \quad (2.8)$$

where Δt is the time step, which is chosen to be 1 day for the simulation model. B_n is taken from historical stream nitrate concentration data provided by Royer et al. (2006) from the Embarras River near Camargo, IL. Daily nitrate concentrations were obtained using linear interpolation of weekly samples. The average $\text{NO}_3\text{-N}$ concentration for the simulation period of June 14, 1993 to March 31, 2003 is 6.79 mg/L. The wetland volume on day n , V_n , is obtained by discretizing equation (2.2) as shown below.

$$V_n = V_{n-1} + [q_n - Q_{0n} + (P_n \times A) - (ET_{C_n} \times A)] \Delta t \quad (2.9)$$

The wetland outflow Q_{0n} is constrained such that the wetland operators seek to maintain a certain target depth (0.5 m in this study). The actual depth of the wetland can fluctuate from day to day depending on environmental conditions. The following overflow model is used to determine the daily wetland outflow:

$$Q_{0n} = \begin{cases} V_{n-1} \Delta t + (q_n + (P_n - ET_{C_n})A) - DA \Delta t & \text{if } V_{n-1} + [q_n + (P_n - ET_{C_n})A] \Delta t > DA \\ 0 & \text{if } V_{n-1} + [q_n + (P_n - ET_{C_n})A] \Delta t \leq DA \end{cases} \quad (2.10)$$

where D is the desired wetland depth. Depending on the previous day's volume and weather, if the inflow and precipitation surpass the evapotranspiration enough on a given day to cause the wetland to exceed its desired depth, the outflow Q_{0n} is the excess water volume. Otherwise, if the wetland is at or below its desired volume the outflow goes to zero. The wetland inflow q_n is determined by the flow availability by the following rule:

$$q_n = \begin{cases} p & \text{if } S_n - l > p \\ S_n - l & \text{if } 0 < S_n - l \leq p \\ 0 & \text{if } S_n - l \leq 0 \end{cases} \quad (2.11)$$

where p is the wetland outflow pumping capacity, S_n is the daily stream flow and l is the instream flow protection limit. For the Embarras River the flow protection limit is taken as the 7-day, 10-year (7Q10) daily low flow from the nearest United States Geological Survey (USGS) site which is $0.0144 \text{ m}^3/\text{s}$. If enough stream flow is available, the inflow for a given day will be the pumping capacity. Otherwise, the inflow is the available streamflow, defined as the difference, when positive, between the daily stream flow and the instream protection limit. The daily stream flow S_n is obtained from historical USGS data. The average stream flow of the Embarras River near Camargo, Illinois for the simulation period is $5.05 \text{ m}^3/\text{s}$.

In order to harvest the wetland biomass, the wetland must be drained annually. To simulate wetland drainage, the wetland inflow and desired depth are set to zero for the time period during which the wetland is drained. Once biomass harvesting is complete, Equations (2.10) and (2.11) continue to describe the wetland outflow and inflow respectively. Nutrient removal by the wetland can be calculated by substituting the above equations into the following:

$$R_n = q_n B_n - Q_{0n} C_n \quad (2.12)$$

where R_n is the wetland mass nitrate removal rate. If equation (2.6) is substituted into equation (2.12), it can be seen that the removal rate is also equal to:

$$R = kAC + \frac{d(VC)}{dt} \quad (2.13)$$

When written in this fashion, it can be seen that the mass $\text{NO}_3\text{-N}$ removal (from the Embarras River) is equal to the rate of change in the amount of nutrients stored in the wetland volume plus the amount of $\text{NO}_3\text{-N}$ transformed via denitrification.

The nutrient removal model does not take into account nutrients stored and released by *Phragmites* biomass. While in actuality the harvesting of biomass would physically remove nutrients from the wetland system, the amount of nutrients removed by plant uptake under ideal flow and nutrient concentration conditions has been shown to account for only about 10% of $\text{NO}_3\text{-N}$ removal in constructed wetland systems, with denitrification being the major nutrient removal pathway (Toet et al. 2005). Furthermore, with a winter harvest, most of the nutrients have been translocated to the rhizomes for

storage during the dormant period, leaving very few nutrients to be removed via above ground plant organs.

2.3. Biomass production and nutrient removal model considerations and interactions

To determine the effect of nutrient removal on biomass production, the daily values of wetland depth and wetland NO₃-N concentration obtained from the nutrient removal model are used as inputs for the biomass production model. In the biomass production model, the net daily photosynthetic production in the i th layer (recall that, for modeling purposes, the aboveground biomass is subdivided in the vertical into stratified 1 cm thick layers) is given by a form of the Michaelis-Menten equation.

$$Ph_{sht}(i) = P_m k_{CO} \tau^{(TC-20)} \frac{I_{PAR}(i)}{K_{PAR} + I_{PAR}(i)} \times \frac{K_{age}}{K_{age} + Age_{sht}} \times \frac{C_{Nitrate}}{K_{Nitrate} + C_{Nitrate}} b_{sht}(i) \quad (2.14)$$

where $Ph_{sht}(i)$ is the photosynthesis of shoots in layer i (g/m²/day) and P_m is the maximum specific net daily photosynthesis rate of the plant top at 20°C in the absence of light and nutrient limitations; k_{CO} is the conversion constant of carbon dioxide to ash-free dry weight; I_{PAR} is the photosynthetically active radiation in the i th layer. Age_{sht} is the age of shoots from the start of growth, $C_{Nitrate}$ is the NO₃-N concentration in the wetland (taken from the nutrient removal model), $b_{sht}(i)$ is the biomass of layer i , τ is the temperature constant and TC is the temperature in Celsius. K_{PAR} , K_{age} , and $K_{Nitrate}$ are the half saturation coefficients of photosynthetically active radiation (PAR), age and nutrient concentration, respectively. The total shoot biomass, B_{sht} , is given by summing the shoot biomass in each layer.

$$B_{sht} = \sum_{i=1}^{i=imax} b_{sht}(i) \quad (2.15)$$

where $imax$ is the index value corresponding to the topmost layer. Michaelis-Menten kinetics assumes that as the nutrient concentration in the wetland increases, net daily photosynthetic production approaches P_m asymptotically (in the absence of temperature, light and age limitations). While, in actuality, nutrient stress can occur if wetland nutrient concentrations are too high, it is assumed that wetland nitrate-nitrogen concentrations do not reach concentrations that would be detrimental to biomass production; therefore only low NO₃-N concentration limitations are considered.

Along with the wetland nutrient concentration, the depth of the wetland is also an input to the biomass production model which is obtained from the nutrient removal simulation model. The depth of the wetland is used to determine rates of photosynthesis for aboveground portions of the plant that are below water. If a layer is below the water surface, there is less light available for photosynthesis due to the tendency of water to reflect or absorb certain wavelengths of light. Moreover, due to shading and scattering, the amount of light that reaches the water surface is severely reduced relative to the amount that reaches the top of the plant. Since the contribution to photosynthetic production by submerged portions of shoots is miniscule due to light limitations, the effect of water depth on biomass production is negligible.

2.4. Cost model

The cost model for the hypothetical system consists of a constructed wetland and a biomass harvesting portion. The constructed wetland cost model describes costs incurred both in the construction and operation of a wetland designed for nutrient removal. The harvesting model takes into account the costs of harvesting the biomass and the potential revenue of biomass sales.

2.4.1. Constructed wetland costs

The two components of wetland costs are capital and operating costs. Since the construction of wetlands is generally site specific, estimates based on local labor and materials are used here. The basic wetland capital cost components for the hypothetical wetland system are:

- Land
- Earthwork
- Liners
- Plants
- Pump and piping

Land costs are estimated from data from the 2005 Land Values & Lease Trends Report which summarizes data obtained by the Illinois Society of Professional Farm Managers and Rural Appraisers (ISPFMRA, 2006). The value chosen for this study is the mean land value for an ‘average productivity’ tract in ‘Region 5’, which includes Ford, Iroquois, Champaign, Vermillion, Douglas, Edgar, and Coles Counties. Land sales information is obtained from Soy Capital Ag Services (soycapitalag.com). Land at the hypothetical site is assumed to cost \$7,549/ha (~\$0.75/m²). In the United States, land purchase prices vary from \$3,000/ha in remote locations with low population density and low agricultural utility to over

\$100,000/ha for land in urbanizing agricultural landscapes (Kadlec & Wallace, 2009). At the end of the wetland project lifetime, the original land purchase is assumed to have a salvage value of 20% of the initial capital outlay. Earthwork costs are estimated to be \$0.86/m² (Waier, 2006). Liner cost and planting costs are estimated to be \$0.64/m² and \$0.86/m² respectively from figures provided by the U.S. Environmental Protection Agency (EPA, 2000). Planting is taken as a one-time initial cost (i.e. no replanting is required). It is assumed that there is an indirect cost of 24% of the initial costs. Indirect costs include permitting, engineering, financing, mobilization, and construction management (Kadlec & Wallace, 2009). In order to have capital costs on the same basis as operating costs, land, earthwork, liner, and planting costs are annualized over an assumed wetland lifetime of 50 years at a discount rate of 7%. Therefore, the capital cost for land, earthwork, liner, and planting, C_W (\$/year) is:

$$C_W = CRF_W \times 1.24A(L + E_1 + E_2 + PL_c) - SFF_W \times 0.2AL \quad (2.16)$$

where L = land cost (\$/m²), E_1 = earthwork cost (\$/m²), E_2 = liner cost (\$/m²), α = wetland area (m²), and PL_c = planting cost (\$/m²). The factors of 1.24 and 0.2 arise from the inclusion of indirect costs and the salvage value of land, respectively. The capital recovery factor (CRF_W) and sinking fund factor (SFF_W) for the constructed wetland are defined as:

$$CRF_W = [A/P, i, L_W] = \left[\frac{i(1+i)^{L_W}}{(1+i)^{L_W} - 1} \right] \quad (2.17)$$

$$SFF_W = [A/F, i, L_W] = \left[\frac{1}{(1+i)^{L_W} - 1} \right] \quad (2.18)$$

where i = interest rate and L_W = wetland lifetime (years). For a project lifetime of 50 years and a discount rate of 7%, $CRF_W = [A/P, 0.07, 50] = 0.0725$ and $SFF_W = [A/F, 0.07, 50] = 0.0025$. In equations (2.17) and (2.18), A does not correspond to the wetland area.

Pump and piping costs, C_P (\$/year), are estimated using data from Peters et al. (2003) using the regression equation:

$$C_P = CRF_P \times 1.736 \cdot \{43883 + 21360(p)^{0.37} + 836[\log(29.4p)]^{3.9}\} \quad (2.19)$$

where p = pumping capacity (m^3/s) and $CRF_p = [A/p, 0.07, 20] = 0.0944$ is the capital recovery factor for the pump and piping. The pump and piping are annualized using an interest rate of 7% and a lifetime (L_p) of 20 years. Inherent in equation (2.19) is the assumption of an installation cost of 40% of total equipment cost, and an indirect cost of 24% of the total initial outlay.

Operating costs include, testing, labor, supplies and power (energy). A significant portion of the overall wetland operation costs come from the cost of the power needed in order to move water through the wetland. In order to estimate the power costs, O_p (\$/year), the following relationship was used:

$$O_p = \frac{H g \rho}{\varepsilon} \gamma \cdot q_{ave} \quad (2.20)$$

where g = acceleration due to gravity (9.81 m/s^2), H = pump hydraulic head (3 m), ρ = density of water (1000 kg/m^3), ε = pump efficiency (80%), γ = electricity rate ($0.046 \text{ $/kWh}$), q_{ave} = average annual inflow (m^3/year). The remaining operation costs associated with testing, labor and supplies (hereafter referred to as operation and maintenance or O&M) are assumed to follow the areal relationship shown below:

$$O_M = OM_c A \quad (2.21)$$

where O_M (\$/year) is the annual operation and maintenance costs. The coefficient OM_c (\$/m²) is taken from data provided by the U.S. Environmental Protection Agency (EPA, 2000). The overall annual wetland cost (\$/year) can be represented by:

$$\text{Annual Wetland Cost} = C_W + C_p + O_p + O_M \quad (2.22)$$

All wetland construction and operating costs are in constant dollar terms. Inflation is not included in the interest rate used in the above calculations.

2.4.2. Harvest operation economics

The two parts of harvesting cost are the cost of harvesting and the revenue from biomass sales. It is assumed that harvesting occurs once a year on January 15, since temperatures are near or below freezing on that date for all years in the simulation period (unlike December 15th or February 15th). Wetland drainage begins a month earlier on December 15th and the wetland is refilled starting on January 30th. In

actuality, harvesting may be performed any time within this 1.5 month window with a negligible difference in biomass since the plant is dormant during this period. However, in order for the harvest to occur the wetland must be drained, the ground must be frozen, and there must be minimal snow. It is assumed that for every simulation year between December 15th and January 30th there exist a few such days during which harvest can occur.

The biomass harvesting is done assuming the same costs as harvesting perennial grasses. Khanna et al. (2008) investigate the costs of producing miscanthus and switchgrass for bioenergy in Illinois. It is assumed that the same equipment and practices can be used to harvest *Phragmites* since the crops are (structurally) similar to each other.

Harvesting *Phragmites* involves the following steps:

- Mowing
- Swathing
- Baling
- Storage

Included in the cost of each of the above components are the costs of machinery, overhead (depreciation, interest, insurance, housing, and repairs), fuel and labor. It is important to note that machinery costs are estimated based on the assumption that the farmer or group co-operating farmers is using own machinery, tractors and harvesting equipment. Per hectare machinery costs are obtained from the Farm Business Management Handbook (Schnitkey et al., 2003a). Not included in the harvesting costs is the transportation of the harvested biomass to a processing facility. In order to estimate transportation costs, distance to a cellulosic ethanol production plant must be known and, since such data are not available, the calculated harvesting costs represent the ‘farm-gate’ costs, although in this case, they include moving the harvested crop 1.62 km to a storage facility. It does not, however, include shipping, handling, marketing, and profit of downstream entities handling the crop.

Previous studies show much variation in the assumptions made about the relation between harvesting costs and biomass yield. It is assumed here that the cost of mowing/conditioning and raking is \$40.52/ha. Mowing and raking is the process of physically cutting the biomass and arranging the cuttings so they can be baled. As with the case of harvesting hay, the cost of baling is yield dependent at the rate of \$15.43/ton of dry matter (Schnitkey et al., 2003b). (Here, tons indicates metric tons.) The cost of renting a tractor, loading it on the field, transporting the bales to the storage area 1.62 km (1 mile) away from the wetland, and unloading and stacking the bales in the storage area is taken as \$7.34/ton of biomass. The most cost-

effective way of biomass storage is outside on crushed rock under a reusable tarp (Duffy & Nanhon, 2002). The cost of storage is \$3.22/ton of biomass as described by Turhollow (2000). Therefore, the harvest cost for year y , H_y (\$), can be described as:

$$H_y = A \times [M_H + Y_y(B_H + O_H + S_H)] \quad (2.23)$$

where A is the wetland area in hectares, M_H (\$/ha) is the cost of mowing/conditioning and raking, Y_y (tons/ha) is the year y yield from the biomass production model, B_H (\$/ton) is the cost of baling, S_H (\$/ton) is the cost of storage and O_H (\$/ton) are the costs associated with renting and loading a tractor on the field, transporting the bales to storage and unloading them.

Quantification of the benefits associated with biomass harvesting proves a difficult task due to the lack of a market price of cellulosic biomass. In order to avoid the simulation of a biomass market, it is assumed that the sale of biomass is based on a contractual agreement between the biomass producer and an ethanol production plant. The processing facility buys biomass from the wetland operator at a constant (farm-gate) price for a certain number of years (i.e. the simulation period). Although sensitivity to biomass price will be examined, for the initial (baseline) scenario the price is taken as \$58/ton which is the farm-gate breakeven price for miscanthus in Illinois as specified by Khanna et al. (2008). Using a constant biomass price for all years gives the following relationship for the year y benefit, B_{ey} (\$):

$$B_{ey} = A \times Y_y \times P_r \quad (2.24)$$

where Y_y is the year y biomass yield (tons/ha), and P_r is the contractual price of the biomass (\$/ton).

Unlike the annualized costs for wetland construction and operation, the harvesting costs and benefits vary from year to year based on the yield. In order to describe the harvesting costs and benefits on an annual worth basis, the present value of $H_y - B_{ey}$ for all 10 years of the simulation period is found and then capital recovery is applied. The annualized harvesting cost can then be found by:

$$\text{Annual Harvest Cost} = CRF_a \times \sum_{y=1}^{SIM} \frac{H_y - B_{ey}}{(1+i)^y} \quad (2.25)$$

where $CRF_a = [A/p, 0.07, 10] = 0.142$ is the capital recovery factor for harvesting costs and benefits, and SIM (years) is the length of the simulation period (10 years in this case). A simulation period of 10 years was chosen because of data limitations (i.e. only 10 years of NO_3 -N concentration data were available for the Embarras River near Camargo, IL). Since the wetland lifetime is 50 years and the pump/piping lifetime is 20 years, the analysis assumes that the weather/stream flow and nitrate load conditions repeat themselves every 10 years during the life of the project. While the assumption of such 10 year cycles is not completely accurate, it is as justifiable as any other alternative built on such a limited data set. It is important to note that for the first year of operation there is no harvest since it is assumed that the crop is not fully established. Also, the assumption is made that only 85% of the total above-ground biomass on the day of harvest can be reaped (i.e. 15% of the biomass is lost during the harvest operation).

The total annualized cost (TC) of a constructed wetland for biomass production is:

$$TC = C_W + C_P + O_P + O_M + CRF_a \times \sum_{y=1}^{SIM} \frac{H_y - B_{ey}}{(1+i)^y} \quad (2.26)$$

2.5. Genetic algorithm optimization

The biomass production, nutrient removal and economic models described above are used to formulate the following multiple objective optimization problem:

$$\text{MINIMIZE } TC = C_W + C_P + O_P + O_M + CRF_a \times \sum_{y=1}^{SIM} \frac{H_y - B_{ey}}{(1+i)^y} \quad (2.27)$$

$$\text{MAXIMIZE } TR = \sum_{y \in SIM} \left(\sum_{n \in N_y} \{R_n\} \right)_y \quad (2.28)$$

subject to:

$$p_l \leq p \leq p_u \quad (2.29)$$

$$0 \leq A \leq A_{\max} \quad (2.30)$$

where N_y is the number of days in year y . The decision variables are the pumping capacity, p (m^3/s), and the wetland area, A (ha). The objectives are the total annual cost, TC (\$/year), and the total nutrient removal for the simulation period, TR (tons). The lower limit of the pumping capacity is constrained by

equation (2.19) to be $0.035 \text{ m}^3/\text{s}$. The upper limit of the pumping capacity, p_u , is chosen to be $57.87 \text{ m}^3/\text{s}$ which corresponds to the 99th percentile of the streamflow during the simulation period. The upper limit of the wetland area (A_{\max}) was chosen as 600 ha which represents about 1% of the Upper Embarras watershed area.

To determine the Pareto-optimal front for the two objectives, the Non-dominated Sorting Genetic Algorithm-II (NSGA-II) was used (Deb et al., 2002). The NSGA-II routine implements a fast non-dominated sorting procedure, elitism for multi-objective search and a parameter-less diversity preservation mechanism. NSGA-II has been applied to multi-objective engineering design problems, and offers better convergence near the true Pareto-optimal front when compared to other elitist multi-objective evolutionary algorithms that pay special attention to creating a diverse Pareto-optimal front (Deb et al., 2002). With only two decision variables and two objectives, NSGA-II promises to deliver consistent results for the problem defined in equations (2.27) through (2.30). The parameters used in the genetic algorithm routine are summarized in the table below:

Table 2.1: Genetic Algorithm Parameters

Parameter	Value
Population Size	100
Number of Generations	100
Crossover Probability	0.8
Mutation Probability	0.5

Because the problem has only two decision variables and two objectives, a large number of generations are not necessary as the algorithm converges quite quickly. Figure 2.2 shows the initial and final populations for the GA optimization using the parameters in Table 2.1. The reason that most individuals in the initial population lie close to the non-inferior set defined by the final generation is that the choice of wetland area (vs. pumping capacity) dominates the system cost, especially for large systems. The difference between the initial and final populations can be more clearly seen in Figure 2.3. The first generation shows a random scatter of points throughout the decision space (as it should), while the final generation shows more of a trend between the two decision variables (especially for smaller systems). The relationships seen in Figure 2.2 and Figure 2.3 are discussed further in the Results section below.

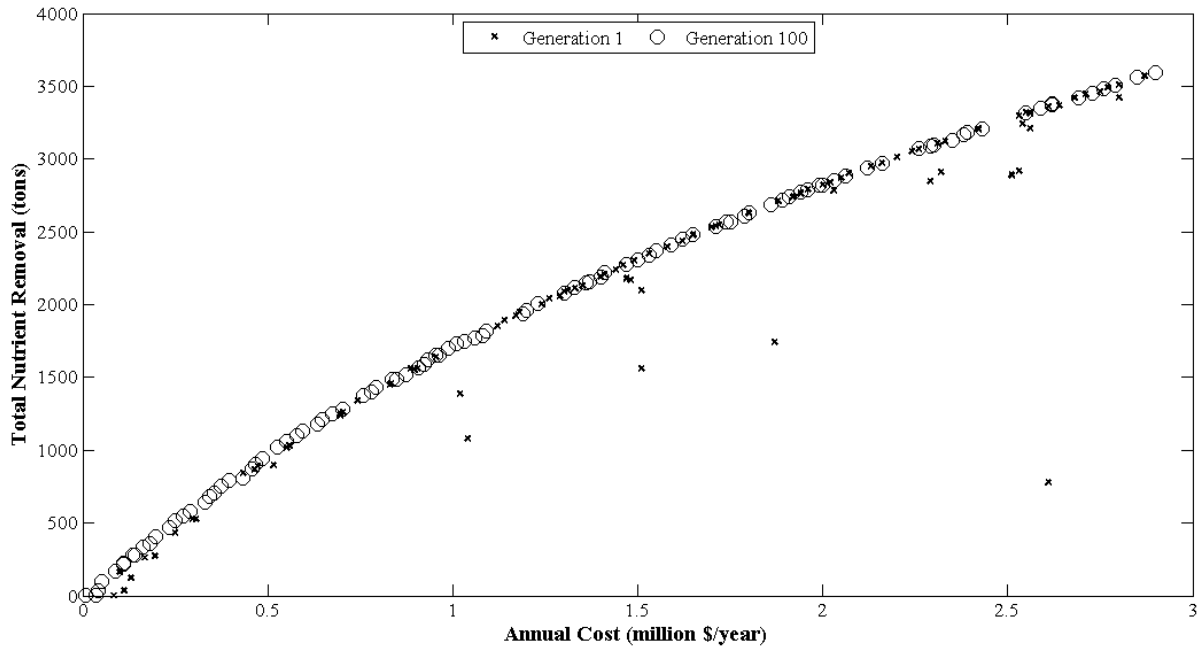


Figure 2.2: Initial (Generation 1) and final (Generation 100) populations from GA optimization showing convergence to the non-inferior set in objective space.

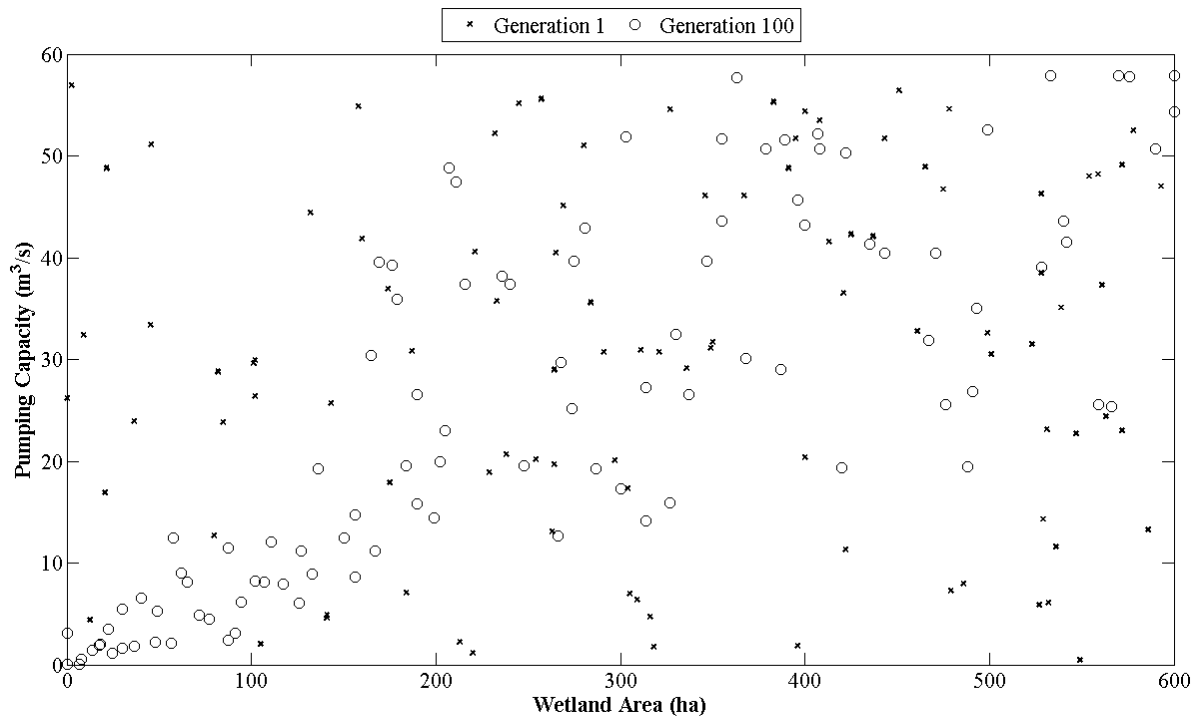


Figure 2.3: Initial (Generation 1) and final (Generation 100) populations from GA optimization showing convergence in decision space.

3. Results

Analysis of the simulation-optimization model described above is carried out in three stages. First, an enumeration approach is used to analyze the simulation model outputs. A discussion of the GA optimization results follows. Finally, the problem is viewed from an efficiency perspective, where minimizing the cost per mass of nutrients removed is treated as the only objective and the total nutrient removal for the simulation period is constrained to be greater than zero.

Since the wetland described in this research is hypothetical, no empirical data exist for the validation of the three simulation models. However, for the highly mechanistic biomass production model, input and output data for a site in central Japan were obtained via a personal communication with Dr. Takashi Asaeda. Using these data, the biomass production simulation model was validated for the central Japanese site. Since the plant growth model is calibrated for various latitudes and climatic regions, the model is assumed to give accurate predictions for biomass production at the hypothetical wetland site near Camargo, Illinois.

In the following sections, the term “baseline scenario” is taken to represent the problem formulation with all parameters and equations as described in the Method section above. This is to differentiate the original model formulation from those of various scenarios that will be introduced in the Discussion section.

3.1. Baseline scenario enumeration results

In order to observe relationships between the cost, nutrient removal and biomass yield with respect to pumping capacity and wetland area, an enumeration approach was used. Several permutations of pumping capacity and wetland area were simulated in order to visualize relationships between the decision variables (viz., pumping capacity and wetland area) and important model outputs. Figure 3.1 is a decision space diagram containing contour plots of both objectives (total nutrient removal and annual cost). The term *total nutrient removal* corresponds to the aggregated total $\text{NO}_3\text{-N}$ removal in tons over the entire simulation period. The optimality conditions correspond to the minimum cost for a given level of required removal, represented by the tangency points between the two families of curves in Figure 3.1. These can be used to determine the optimal expansion path, the locus of all such tangency points which is also shown in Figure 3.1. The entire range of wetland area and pumping capacity is not shown in the figures below in order to show more detail for the range where the curves show the most interesting behavior.

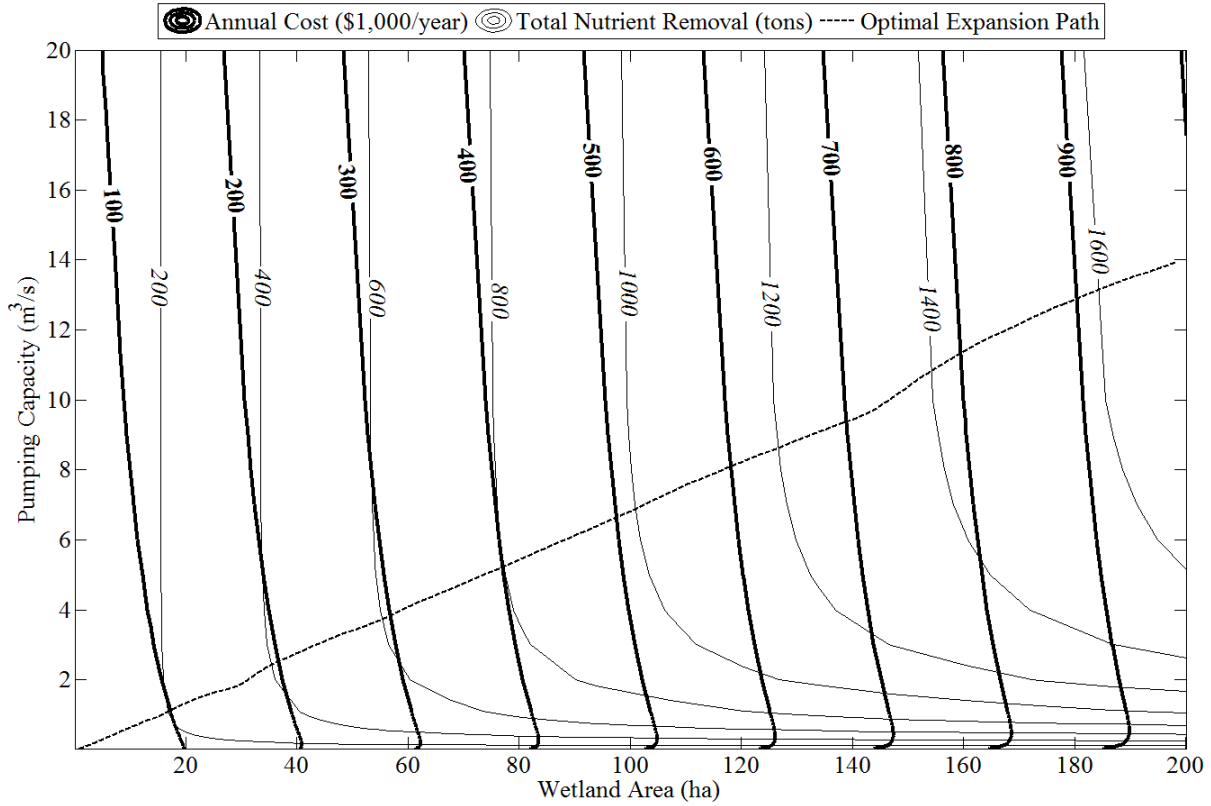


Figure 3.1: Contour Plots of Objectives in Decision Space

The total nutrient removal of the wetland is mainly governed by the amount of nutrients pumped into the wetland (nutrient throughput) and the amount of time that the nutrients spend in the wetland (hydraulic residence time). The relationship between the nutrient throughput and the hydraulic residence time (HRT) is illustrated by the family of constant nutrient removal curves in Figure 3.1. It is important to note that there is a volumetric wetland flow throughput limit which is dictated by the streamflow and weather conditions (refer to Equations 2.10 and 2.11). The design pumping capacity limits the nutrient throughput of the wetland on a given day, and the choice of wetland area determines the HRT. Figure 3.2 shows the cumulative distribution function for the available streamflow during the simulation period. Alternatively, the axes in Figure 3.2 could be labeled “design pumping capacity” (x-axis) and “percent of days for which all available streamflow may be captured during the simulation period” (y-axis). For example, if the design pumping capacity is chosen as $2 \text{ m}^3/\text{s}$, then any day where the available streamflow is equal to or less than $2 \text{ m}^3/\text{s}$ all of the available flow will be pumped through the wetland. For days where the available flow exceeds $2 \text{ m}^3/\text{s}$, the amount of water pumped into the wetland is limited by the pumping capacity, as opposed to being limited by the streamflow (see Equations 2.10 and 2.11). From Figure 3.2, it can be seen that about 57% of the time, the available streamflow is $2 \text{ m}^3/\text{s}$ or less, meaning that on 57% of

the days in the simulation period, all of the available flow is pumped in to the wetland. On all of the other days, the streamflow is greater than $2 \text{ m}^3/\text{s}$, but water can still only be pumped at a rate of $2 \text{ m}^3/\text{s}$ into the wetland. If the pumping capacity is increased to $10 \text{ m}^3/\text{s}$, then all of the available streamflow (and associated nutrients) can be captured for 86% of the days within the simulation period. As the design pumping capacity becomes larger, the amount of days for which the available flow exceeds the pumping capacity becomes less until all available flow is pumped into the wetland (at a pumping capacity of about $200 \text{ m}^3/\text{s}$). Above a pumping capacity of $30 \text{ m}^3/\text{s}$, the difference in the amount of streamflow captured is negligible because there may only be a handful of days (corresponding to extreme events) for which the available flow exceeds $30 \text{ m}^3/\text{s}$ and pumping water on these days will have a negligible effect on the total amount of flow and nutrients provided to the wetland during the simulation period.

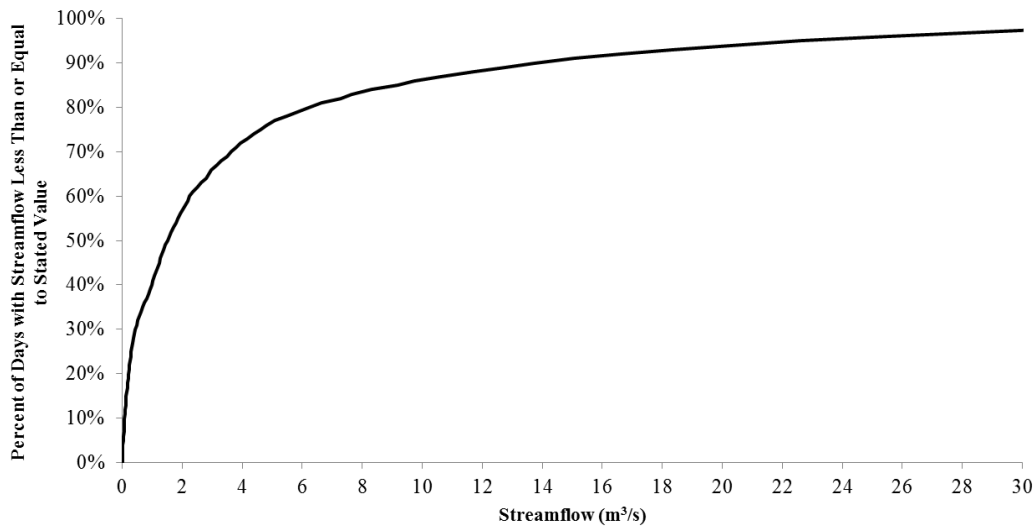


Figure 3.2: Cumulative Distribution of daily streamflow for the simulation period for the Embarras River near Camargo, IL

The sharp initial rise of the curve in Figure 3.2 explains the large increase of nutrient removal in response to an increase in pumping capacity at low pumping capacities, because more nutrients are provided to the wetland per unit increase of pumping capacity. For high pumping capacities, the only way to improve nutrient removal is to increase wetland area since a unit increase in pumping capacity provides only a small increase in the amount of nutrients provided to the wetland. For smaller pumping capacities, a unit increase may deliver significantly more nutrients to the wetland, but if the wetland is small the removal will be low due to a short HRT. Therefore, for low pumping capacities, it is the combination of wetland area and pumping capacity that decides the removal, while for large pumping capacities the wetland area becomes the key factor in determining the total nutrient removal because the amount of nutrients being delivered to the wetland approaches the maximum available from the river. This is illustrated in Figure

3.1 by the verticality of the total nutrient removal contours as pumping capacity increases, and the increase in the minimum pumping capacity associated with the transition to verticality as the wetland area increases.

The contours of overall cost of the wetland system are the bold lines in Figure 3.1. The fact that the cost contours are nearly vertical indicates a stronger dependence of overall cost on wetland area than on pumping capacity. The influence of biomass harvesting and sales, wetland area and pumping capacity on the overall cost of the wetland can be seen in Figure 3.3.

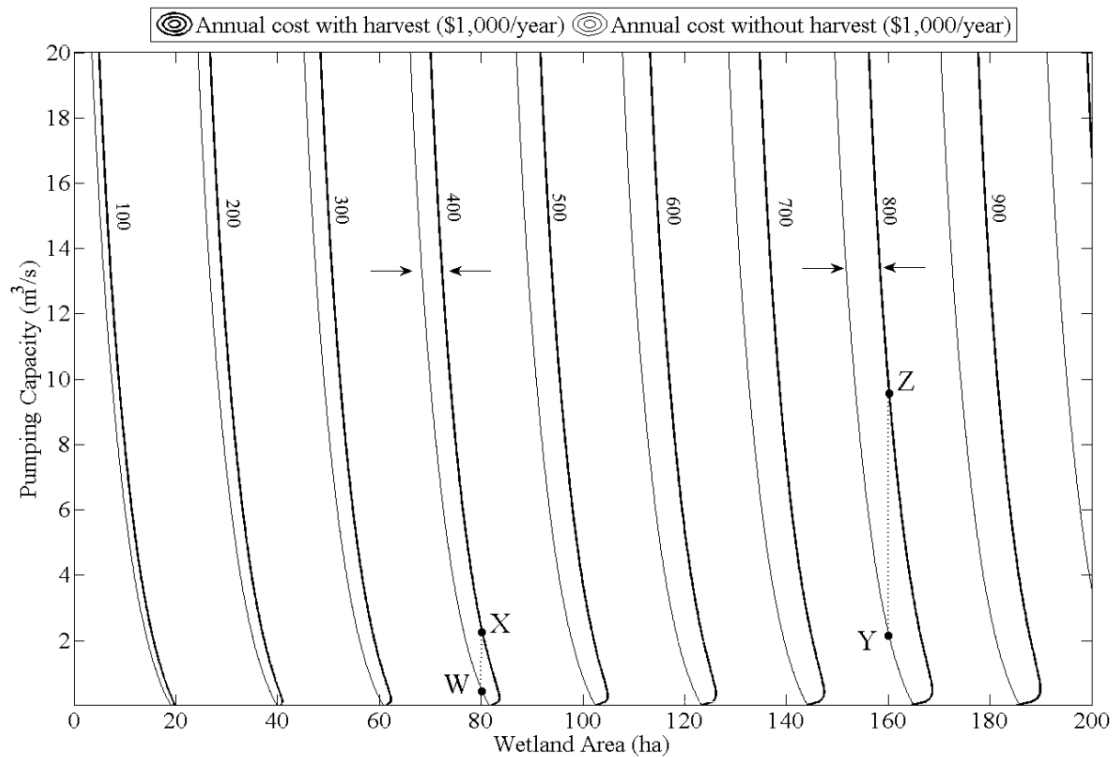


Figure 3.3: Comparison of annual costs when costs and benefits associated with harvesting are included (bold) and not included (light). Each label corresponds to the two cost contours to its immediate left.

This figure compares the cost contours between the Baseline scenario and a scenario where the costs and benefits associated with harvesting are neglected (a more complete description of the scenario can be found in section 4 where the “NoHarvest” scenario is described). In the latter case, all of the contour lines in Figure 3.3 exhibit monotonic behavior showing that in order to maintain a constant wetland cost, the area must decrease and the pumping capacity must increase along the contours shown. When the effect of biomass harvesting is considered, the curves display a different behavior for smaller pumping capacities, which is shown in detail in Figure 3.4. When the pumping capacity is very small and wetland area is large (point A), the amount of nutrients supplied to the wetland is not enough to support the large crop stand,

causing the plant to be stressed and to produce less biomass (see section 2.3), leading to less revenue from biomass sales.

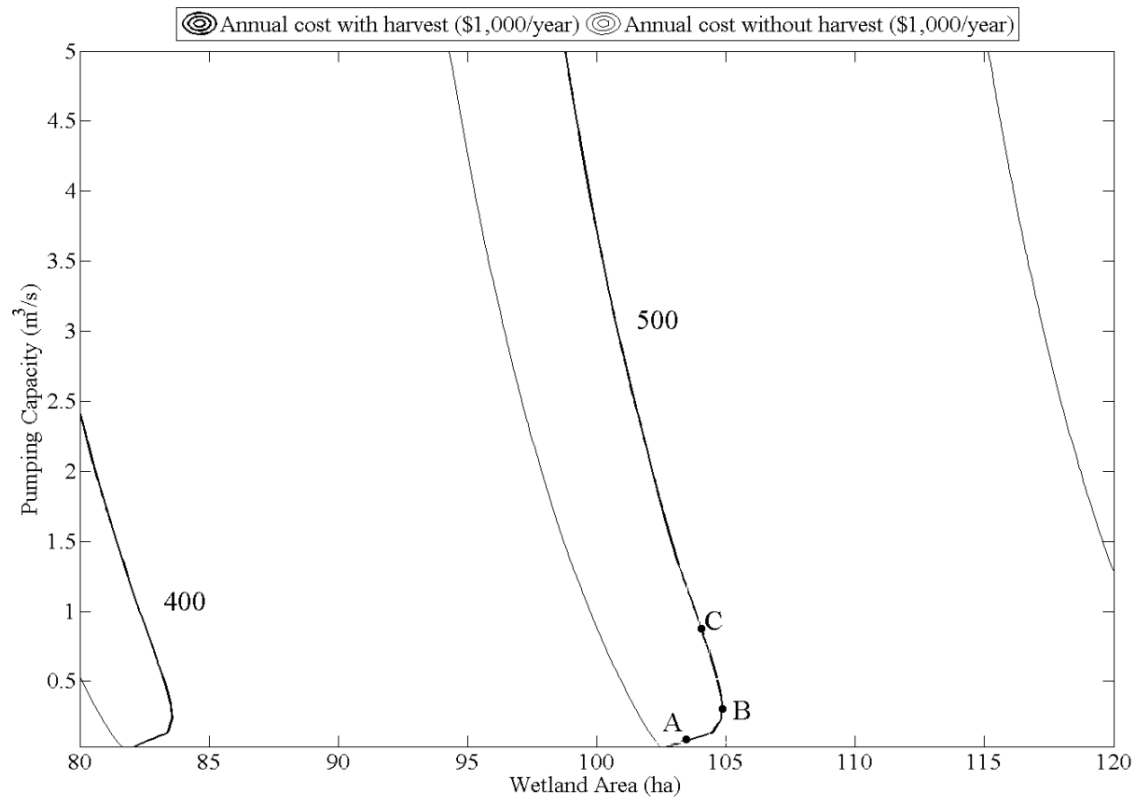


Figure 3.4: Detail of Figure 3.3

In moving from point A to point B along the contour, the small increase in pumping capacity affects the biomass production (by supplying more nutrients to the wetland) to such a point that in order to offset the revenue collected from biomass sales, there must be an increase in the wetland area so that both points have the same annual cost associated with them. The reason that changing the pumping capacity the slightest bit causes such an increase in biomass production is because significantly more nutrients are delivered to the wetland causing the crop to be stressed less of the time. As discussed above and shown in Figure 3.2, for low pumping capacities a unit increase in pumping capacity results in being able to pump all available flow for significantly more days during the simulation period, which is associated with being able to supply more nutrients to the *Phragmites* crop. As the pumping capacity is further increased from B to C, supplying more nutrients to the wetland does not have such a profound effect on the biomass yield because sufficient nutrients are being supplied that nutrient stress is becoming less of a factor when determining biomass production, as shown by the vertical asymptotes in Figure 3.5. Figure 3.5 shows the relationship between wetland area, pumping capacity and biomass production (production = yield \times area) for the last year of the simulation period *only* (referred to here as the total year 10 biomass production). It

can be seen that the contours in Figure 3.5 exhibit a similar pattern as the total nutrient removal contours (Figure 3.1) in their verticality at high pumping rates and the increase in transitional pumping rate with increasing wetland area. This reinforces the idea that high levels of nutrient removal are associated with lower nutrient concentration in the wetland water and soil, and thus, lower biomass production per unit area due to nutrient stress. As biomass production reaches its maximum for a given area, the cost of increasing the pumping capacity will need to be offset by diminishing the size of the system, causing both sets of curves in Figure 3.3 to exhibit the same behavior for pumping capacities greater than $4 \text{ m}^2/\text{s}$.

Another way to look at figure 3.3 is from the perspective of a decision maker who has a given budget and must decide between setting up a wetland with or without a harvesting operation. If, in addition to constraining the cost, the pumping capacity is also constrained, Figure 3.3 shows that a larger wetland can be constructed if a harvesting operation is considered. The horizontal gap between contours of the same cost and different operational considerations (i.e. harvest vs. no harvest) increases as the area increases (this is shown by the arrows in Figure 3.3). The reason for this increasing gap size is related to the relationship seen in Figure 3.5 between wetland area and maximum biomass production. A unit increase in area has more of an effect on the maximum biomass production (the vertical asymptotes in Figure 3.5) for small areas than for large ones. Above a pumping capacity of about $5 \text{ m}^3/\text{s}$, an increase in area removal is associated with an increase in nutrient removal (see Figure 3.2). Although there is nutrient stress (i.e. lower *per unit area* biomass yield) associated with high nutrient removal levels (i.e. low wetland $\text{NO}_3\text{-N}$ concentration), the effect of nutrient limitations on the *per unit area* biomass yield is not sufficient enough to cause a decrease in total biomass production (yield \times area) as the wetland size becomes larger. Therefore, increasing the wetland size produces more total biomass, a trend that is more prominent for lower wetland areas and is depicted by the increase in spacing of the vertical asymptotes in Figure 3.5.

On the other hand, if the decision maker is constrained by the cost of the project and the wetland area, there is a difference in the design pumping capacity between the baseline scenario and the scenario where harvesting costs and benefits are neglected (see NoHarvest scenario below in Section 4). Line segments WX and YZ in Figure 3.3 show the difference in pumping capacities for two levels of cost. As was the case with the horizontal gaps between the contours in Figure 3.3, the vertical gaps also increase as the wetland becomes larger. The vertical gaps have the same implications as the horizontal gaps, where if the wetland is harvested, a larger pump can be chosen since the cost will be offset by biomass sales. The vertical differences show a more pronounced trend than the horizontal gaps because the pump/piping related costs are less significant than area-related costs.

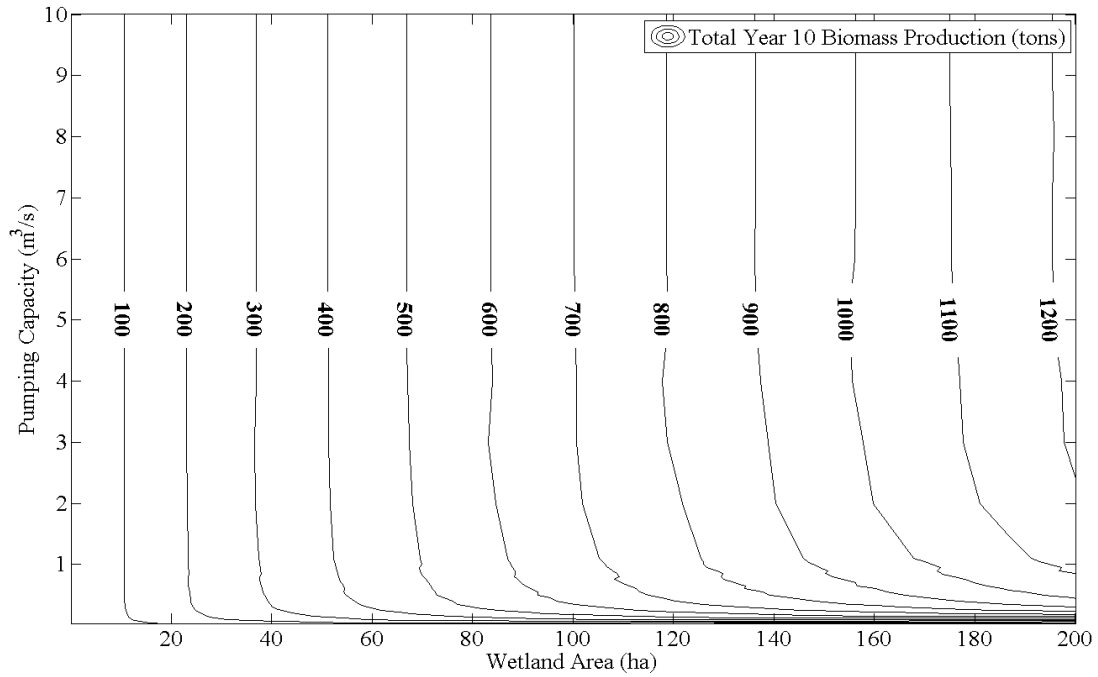


Figure 3.5: Contour plot in decision space of total biomass production in the last year of the simulation period.

3.2. Baseline scenario genetic algorithm results

After assessing the relationships between key model inputs and outputs by enumeration, the overall wetland simulation model was linked to the NSGA-II genetic algorithm routine in order to help visualize the Pareto-optimal frontier between cost and nutrient removal (i.e., in objective space). Figure 3.6 shows the Pareto optimal frontier as determined by the GA optimization as well as the results determined by enumeration. The fact that the data points obtained from enumeration appear to form lines stems from how the decision variables were discretized in the enumeration analysis (note that the decision variables were treated as continuous in the GA optimization). Every vertical “line” in Figure 3.6 represents the evaluation of the objectives for a single value of area over a range of pumping capacities (not all enumeration results are shown in Figure 3.6 to promote visual clarity). Each point on the Pareto-optimal frontier (as determined from GA simulation) represents an optimal combination of wetland area and pumping capacity with respect to the two objectives. Furthermore, the Pareto-optimal frontier is the boundary between the set of infeasible and feasible-but-inferior solutions, with the latter lying below the curve. The fact that the GA simulation results form an envelope around the enumeration results gives

confidence that the GA optimization is indeed converging to a global optimum. In essence, the Pareto frontier represents the maximum feasible amount of nutrient removal for a given cost, e.g., for a limited budget. Alternatively, it represents the minimal cost for a required nutrient removal task. Once the point on the non-inferior set is known, the optimal combination of wetland area and pumping capacity can be located as the point on the optimal expansion path (Figure 3.1) corresponding to the contour line for either total nutrient removal or cost.

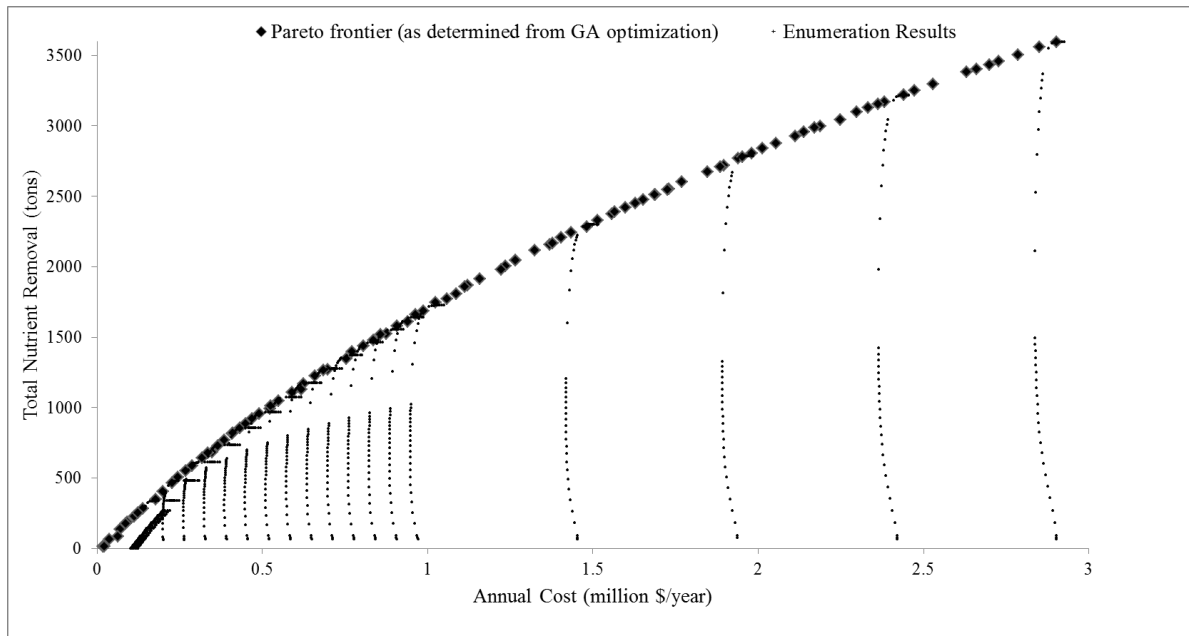


Figure 3.6: Pareto frontier and enumeration results for the baseline scenario

It is apparent from Figure 3.6 that there is no combination of wetland area and pumping capacity that would yield a negative annual cost (i.e. profit). The monotonicity of the Pareto frontier stems from the fact that in order to increase removal, either the pumping capacity (nutrient throughput) or wetland area (HRT) must be increased, which results in a more expensive system. The Pareto frontier shows an asymptotic behavior as cost increases in that there is a theoretical maximum amount of nutrients that can be removed. This behavior can be seen if the upper bounds on the wetland area and pumping capacity are increased to 48200 ha and 200 m³/s, respectively. These upper bounds represent the entire area of the Upper Embarras Watershed and the maximum daily streamflow during the simulation period.

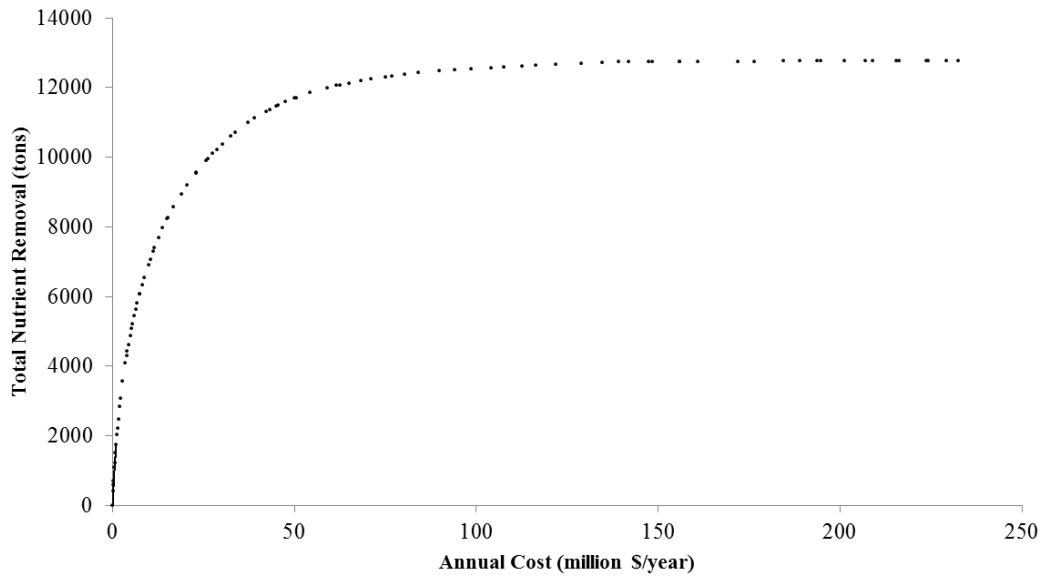


Figure 3.7: Pareto optimal frontier as determined by GA simulations where the maximum possible area and pumping capacity are 48,200 ha and 200 m³/s, respectively.

Figure 3.8 shows the Pareto frontier as determined by GA simulation as well as the corresponding wetland area and pumping capacity for each individual in the final generation. Moving along the Pareto frontier from low annual cost to high annual cost, there is a clear linear relationship between the wetland area and cost. However such a strong trend is not shown by the pumping capacities. As noted earlier, this is because the choice of pumping capacity has more of an effect on removal and cost when the wetland area is small. As the area increases, the choice of pumping capacity has less effect on the nutrient removal and cost. Once the pumping capacity reaches a value of about 10 m³/s, any increase will provide only slightly more nutrients to the wetland, thus providing only a small increase in removal. Furthermore, as the area increases along the Pareto frontier, the cost associated with a given pumping capacity represents less of the fractional cost of the project. Figure 3.9 shows a contour plot of the percentage of the annual cost that is attributed to pump/piping costs (for the baseline scenario) along with the (baseline) optimal expansion path. Looking at the optimal expansion path (which shows the Pareto frontier in decision space), it can be seen that pumping and piping costs make up a larger percentage of the optimal total annual cost for small wetland areas than for larger areas. Because the total cost of the system depends less on the chosen pumping capacity, as the area increases, pumping capacity may vary substantially without significantly affecting the total cost of the system.

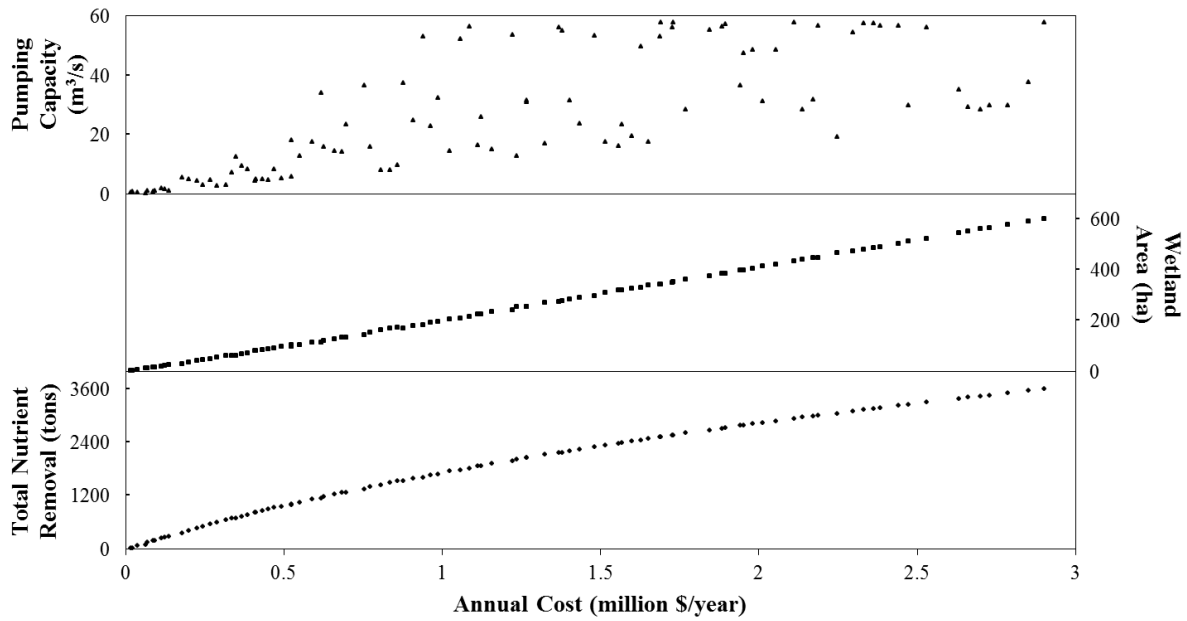


Figure 3.8: Wetland areas and pumping capacities for the Pareto optimal frontier, baseline scenario.

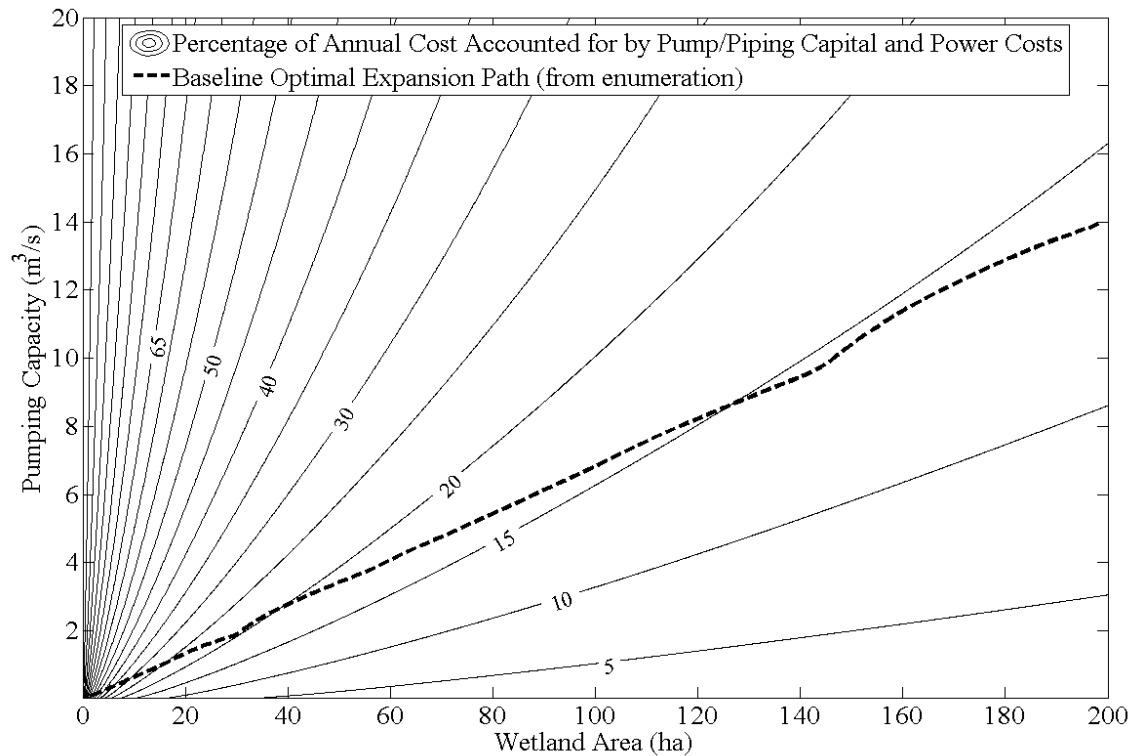


Figure 3.9: Contour plot showing the fraction of the total annual cost (%) that arises from capital and operation costs associated with pumping and piping and the optimal expansion path for the baseline scenario.

3.3. Baseline scenario cost-per-removal results

Apart from the examination of tradeoffs between cost and nutrient removal, the constructed wetland design problem may be regarded from a cost-per-removal perspective, the rationale for which is twofold. The cost per kilogram of $\text{NO}_3\text{-N}$ removal is a common way of characterizing removal cost, allowing a more acceptable basis of comparison with conventional—and other unconventional—techniques. Furthermore, with a price on nitrogen removal, the implications and limitations of a wetland treatment system designed for biomass production can be viewed from a nitrogen trading perspective (assuming the existence of a nitrogen discharge market). The average annual removal is divided by the annual cost to obtain a measure of annual cost per average amount of N-NO_3 removed, referred to here as “cost-per-removal”. Figure 3.10 shows the contours that represent constant levels of cost-per-removal in decision space for the baseline scenario.

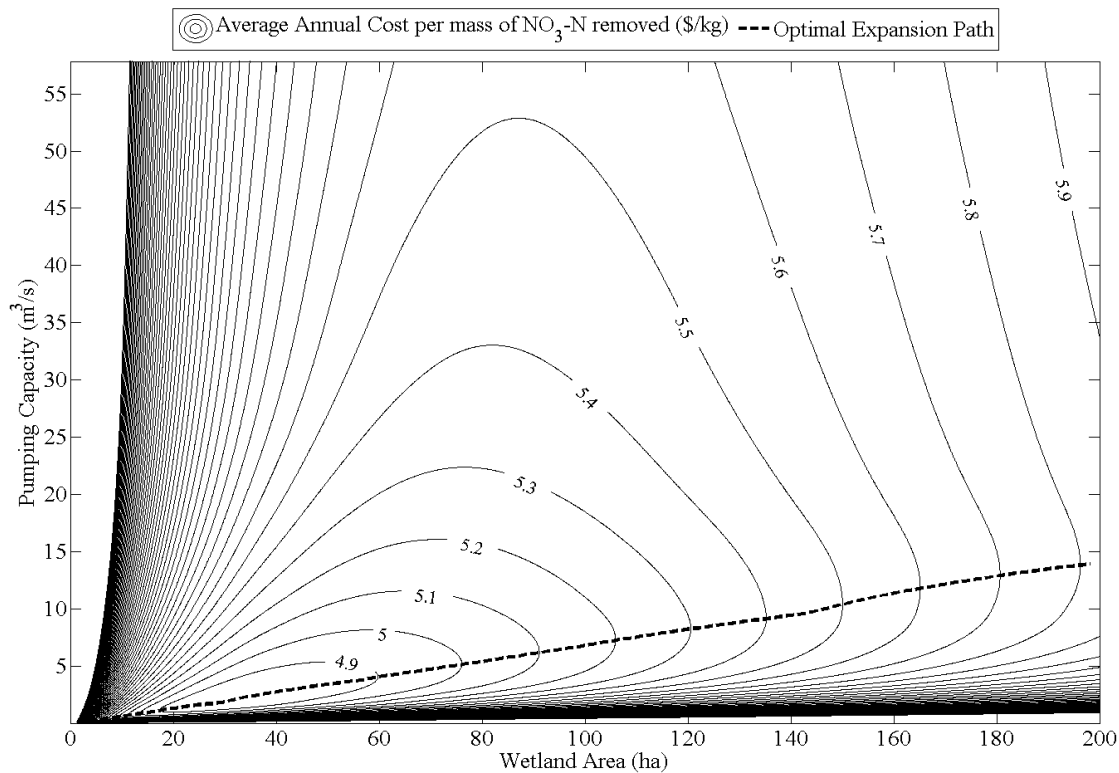


Figure 3.10: Contour plot of cost-per-removal and optimal expansion path in decision space for the baseline scenario.

The shapes of the contours in Figure 3.10 show that for a required level of cost efficiency, there is a maximum area and a single associated pumping capacity. However, for wetland areas smaller than this maximum, there are two values of pumping capacity that give the same cost efficiency. The two points

correspond to either a high nutrient throughput (high pumping capacity) or a high hydraulic residence time (low pumping capacity). Figure 3.11 shows the minimum cost-per-removal as a function of the wetland area, as determined by the baseline enumeration results. In order to determine the global minimum cost per removal, a single objective GA simulation was run with the objective being to minimize the cost-per-removal. The minimum cost-per-removal, as determined by the GA simulation, is determined to be \$4.8/kg NO₃-N removed which corresponds to an area of 33.8 ha, a pumping capacity of 2.28 m³/s, an annual cost of \$185,366 and a total nutrient removal of 386 tons for the simulation period.

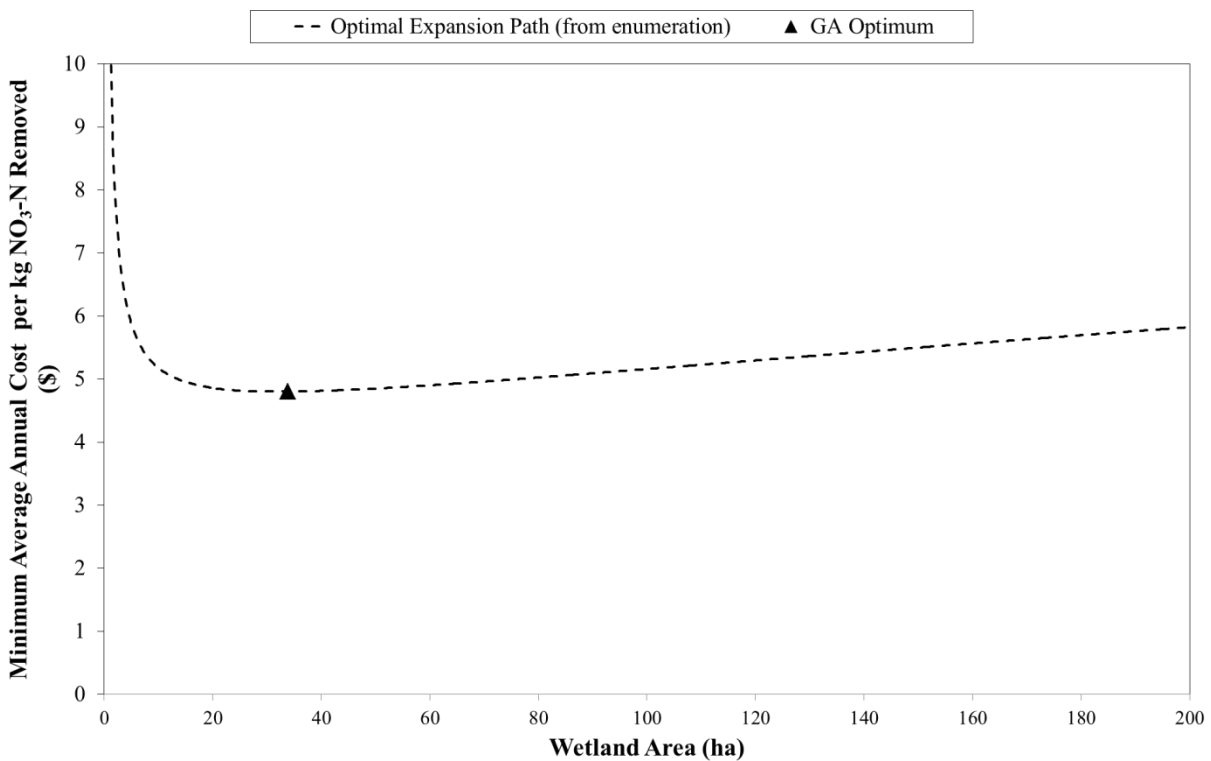


Figure 3.11: The optimal expansion path as determined from enumeration, and the global minimum cost-per-removal from GA optimization.

4. Discussion

To assess how capital costs, operation costs and benefits from biomass sales affect the Pareto frontier, the following scenarios were created by altering the parameters presented in the economic model description:

NoHarvest: In this scenario, the constructed wetland is assumed to be constructed and operated as a wetland designed *only* to treat water quality. For this scenario, the wetland is assumed not to be harvested or drained at any point in the simulation period. Furthermore, any costs or revenue associated with biomass harvesting are neglected in the simulation.

NoLand: For this scenario the cost of purchasing land on which to construct the wetland is neglected. Leaving out the cost of land can be justified by assuming one of several possible land tenure scenarios by which land may be viewed as a sunk cost. For example, landowners who have institutional or cultural restrictions against selling land, who have owned a plot of land for a long time, or have obtained a plot through inheritance may have reason to disregard the cost of land.

NoPump: In this scenario, it is assumed that the wetland is a ‘passive’ system and is constructed in a way such that natural flow through the system is possible. The pumping/piping capital cost as well as the power costs associated with running the pump is assumed to be zero. Although the idea of a passive system is attractive, much uncertainty is introduced when it comes to the wetland throughput and therefore effecting the total nutrient removal. Moreover, piping, valve, and labor costs would still have to be incurred.

NoPlant: This scenario assumes that the cost of initially planting the wetland is zero. Allowing local native wetland plants to naturally populate the wetland is an option to establish vegetation. In constructed wetlands, drawbacks of natural recruitment include a longer establishment time and not having control over what type of vegetation colonizes the wetland.

NoCapNoOM: Not all costs associated with the establishment of the wetland are included in the analysis. All pump/piping and power costs are still included. In this scenario, the land on which the wetland is to be constructed is assumed to have once been a natural wetland that has incurred a change in local hydraulic conditions. The assumption is made that with the installation and operation of a pump and piping system, the wetland would operate normally without any capital costs associated with building the wetland system.

SoyPrice: In this set of circumstances, the contractual price for the sale of cellulosic biomass is assumed to be the same as the average 1997 Illinois soybean price. Although it is not foreseeable that cellulosic biomass would be valued at such a high price, this scenario provides an example of an extreme situation. The soybean price data was provided by the University of Illinois Extension's farmdoc website.

Baseline: This scenario uses the data upon which Figure 3.1 and Figure 3.5 are based, and includes all costs and the biomass price of \$58/ton as determined by Khanna et al. (2008).

Table 4.1 outlines the different cost scenarios based on which parameters are altered and Figure 4.1 shows the Pareto frontiers for the scenarios outlined.

Table 4.1: Economic model parameters for different cost scenarios

	Parameters								
	L (\$/m ²)	E_1 (\$/m ²)	E_2 (\$/m ²)	PL_c (\$/m ²)	P_r (\$/ton)	C_p (\$/year)	O_p (\$/year)	OM_c (\$/m ² /year)	H_y (\$/year)
Baseline Value	0.75	0.86	0.64	0.86	58	Eq. (2.19)	Eq. (2.20)	0.2	Eq. (2.23)
NoHarvest*	0.75	0.86	0.64	0.86	0	Eq. (2.19)	Eq. (2.20)	0.2	0
NoLand	0	0.86	0.64	0.86	58	Eq. (2.19)	Eq. (2.20)	0.2	Eq. (2.23)
NoPump	0.75	0.86	0.64	0.86	58	0	0	0.2	Eq. (2.23)
NoPlant	0.75	0.86	0.64	0	58	Eq. (2.19)	Eq. (2.20)	0.2	Eq. (2.23)
NoCapNoOM	0	0	0	0	58	Eq. (2.19)	Eq. (2.20)	0	Eq. (2.23)
SoyPrice	0.75	0.86	0.64	0.86	277.42	Eq. (2.19)	Eq. (2.20)	0.2	Eq. (2.23)
*for the NoHarvest scenario, it is assumed that the wetland is not drained for harvesting, which is reflected in the simulation formulation									

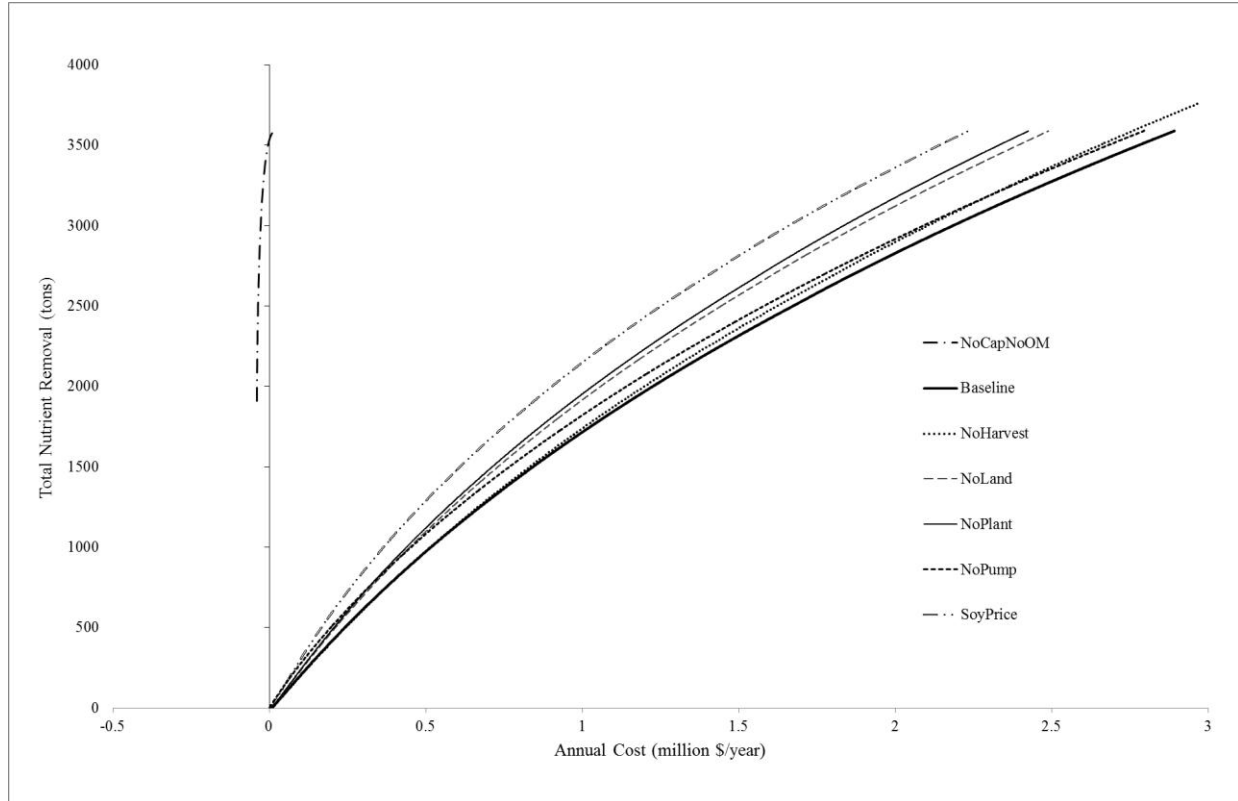


Figure 4.1: Pareto-optimal frontiers for various cost scenarios

Under the NoLand and NoPlant scenarios, the low cost curves follow the baseline and gradually show a higher removal for a given cost when compared to the baseline as the cost increases. This relationship shows that lower levels of required removal are influenced more by the choice of pumping capacity than wetland area and vice versa for higher required removal levels. The relationship between the NoLand and NoPlant scenarios and the baseline can be further explained by the fact that land and planting costs are directly proportional to the wetland area. On the other hand, the Pareto front for the NoPump scenario shows a larger cost discrepancy (for a given level of removal) for low required removal levels when compared to the baseline. For removal levels less than 1000 tons, NoPump provides a cheaper alternative even when land or planting costs are not considered. The Pareto front for the NoPump scenario illustrates the importance of the cost of pumping/piping for lower nutrient removals (which is detailed in Figure 3.9). The SoyPrice scenario shows similar behavior as the NoLand and NoPlant scenarios given that revenue from biomass sales is proportional to the wetland area as well as the biomass production. It can

be seen that even with an unrealistically high price for biomass, the wetland is still not profitable as long as land and operation incur a cost.

The NoHarvest scenario allows for the comparison between the system in question and a constructed wetland for nutrient removal only. From Figure 4.1 it can be seen that the Pareto frontier for the NoHarvest scenario closely follows the Baseline for low wetland costs, and begins to show deviation at an annual cost of about \$1 million/year. The fact that the revenue from biomass sales is quite small compared to capital costs is the reason that the NoHarvest and Baseline scenarios show similar Pareto frontiers for low project costs. The discrepancy between the NoHarvest and Baseline Pareto frontiers for higher annual costs arises from the effect of draining the wetland. During the 1.5 month period when the wetland is drained for harvesting there is no nutrient removal since the wetland inflow is constrained to be zero. Therefore, when the wetland is not drained, there is a higher nutrient throughput and an associated higher potential for removal. However, this potential cannot be realized if the wetland is too small or the pumping capacity is too large which results in the NoHarvest Pareto frontier to deviate noticeably from the Baseline only when the annual cost (i.e. area) is higher. It is important to note that the removal of biomass has both advantages and disadvantages when denitrification and wetland cost are considered. At the end of the growing season, the remaining harvestable aboveground biomass is referred to as 'standing dead' since at this point all of the nutrients have transferred to the rhizomes leaving only the shoots and panicles of the plant as deceased plant matter. In a natural system, the standing dead would remain into the following season until eventually most of the biomass falls back into the wetland as litter and decomposes. Dead or decomposing biomass plays a role in denitrification by providing a primary substrate for microbial denitrification. However, large amounts of litter can be detrimental to both the next season's biomass production as well as maintaining flow through the wetland. While the effect of standing dead on denitrification rates and wetland flow is not considered in the simulation models, it is expected that the denitrification rate constant (k) could be different for the NoHarvest scenario. Furthermore, it may be possible that more costs could be associated with the maintenance of the wetland in the NoHarvest scenario since it may be necessary to clear some biomass in order to maintain a certain nutrient removal or flow rate through the wetland.

In addition to the scenarios outlined in Table 4.1, various combinations of the scenarios (e.g. NoLandNoPump would correspond to a scenario where the cost of land *and* the cost of pump/piping are not included) were also run through the GA model and did not result in any wetland area and pumping capacity combinations that produced a negative annual cost (i.e. profit). Only when the capital and

operating costs of constructing the wetland were neglected in the NoCapNoOM scenario (see Table 4.1), were profits seen in the operation of the wetland.

Figure 4.2 depicts a similar plot as Figure 3.8 for the NoCapNoOM scenario. Since major area-dependent capital and operating costs are neglected in the NoCapNoOM scenario, it follows that the GA would converge to a solution where each optimal combination of wetland area and pumping capacity has the area at its maximum. The pumping capacity as cost increases shows a clearer trend than in the baseline scenario which is once again directly related to the cumulative distribution of the streamflow shown in Figure 3.2 where deviations in low magnitude pumping capacities result in larger changes in nutrient removal as compared to similar deviations for large magnitude pumping capacities. Even when the major costs associated with wetland construction are neglected, only a maximum annual profit of about \$40,000 is achieved.

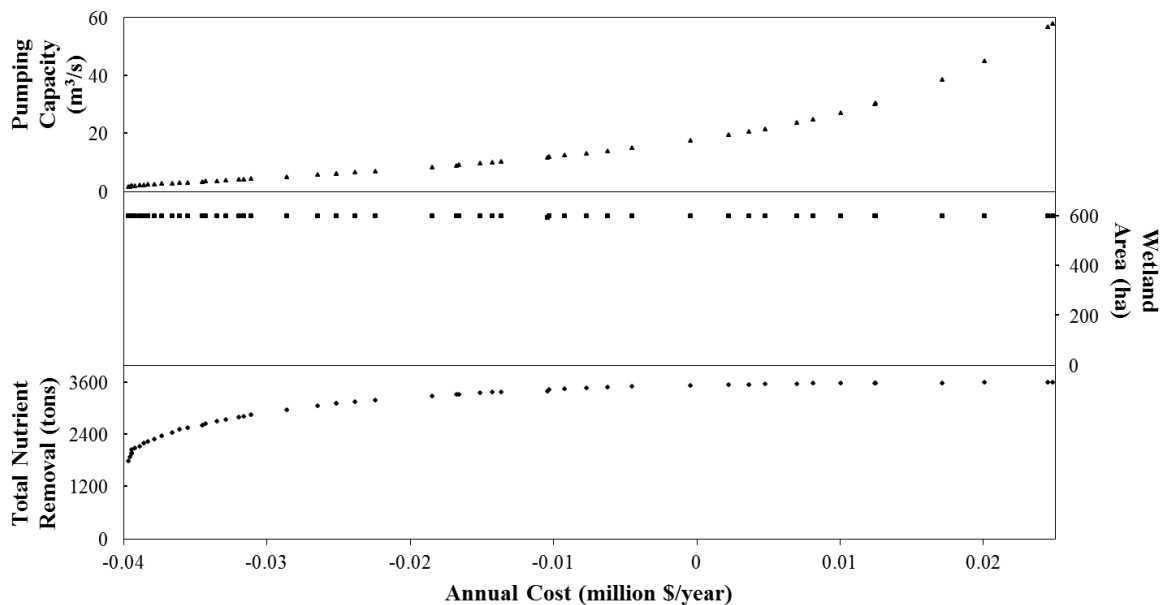


Figure 4.2: Pareto optimal frontier and corresponding wetland areas and pumping capacities for the NoCapNoOM scenario.

As with the baseline scenario, optimal costs were expressed as cost-per-removal, in addition to the Pareto frontier as obtained from GA optimization. Figure 4.3 shows the maximum cost efficiency (minimum cost per kg removed) as a function of wetland area for all of the cost scenarios. It can be seen that for the Baseline, NoHarvest, NoLand, NoPlant, and SoyPrice scenarios, the curves in Figure 4.3 exhibit a local

minimum, while for the NoCapNoOM and NoPump scenarios, they are monotonically decreasing and increasing, respectively.

Table 4.2 shows the optimal area, pumping capacity and corresponding annual cost, total removal and cost-per-removal for all of the scenarios. For the scenarios with nonmonotonic curves in Figure 4.3, the optimal wetland area and pumping capacity are all relatively similar yielding a wetland area between 29.1 ha and 37 ha and a pumping capacity in the range of 1.5 m³/s to 2.3 m³/s. The similarity of the optimal cost-per-removal values arise due to the fact that in each of the scenarios, the annual cost is only slightly altered when changing parameters from scenario to scenario (this can also be seen in the tight bunching of curves in Figure 4.1).

The shape of the NoPump curve shows the importance of the cost of pumping for small wetlands. Since the annual project cost is dominated by pumping/piping costs for small wetlands (see Figure 3.9), it follows that the most cost efficient wetland will be small (in this case as small as possible) in order to take advantage in the omission of pump/piping costs in the NoPump scenario. In the NoCapNoOM scenario, increasing the wetland area has a small effect on the cost since the capital and O&M costs (which are omitted in this case) for the wetland are highly dependent on the area of the system. Therefore, without a large cost penalty for increasing the wetland size, the largest wetland possible will show the lowest cost-per-removal.

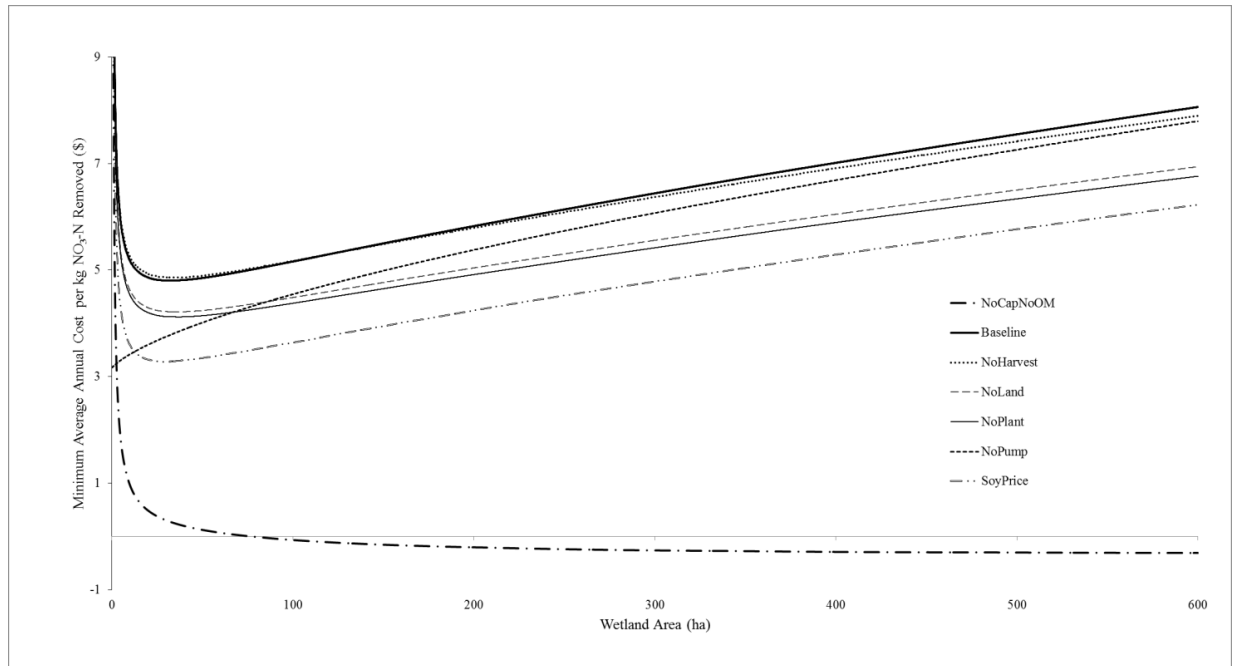


Figure 4.3: Minimum cost-per-removal as a function of wetland area as determined from enumeration for various cost scenarios.

Table 4.2: Optimal cost-per-removal wetlands for cost scenarios

	Wetland Area <i>ha</i>	Pumping Capacity <i>m³/s</i>	Annual Cost <i>million \$/year</i>	Total Removal <i>tons</i>	Cost-per- Removal <i>\$/kg NO₃-N/year</i>
Baseline	33.8	2.3	0.19	386	4.80
NoCapNoOM	600	0.5	-0.03	870.44	-0.31
NoHarvest	35	2.3	0.20	413.76	4.86
NoLand	36.4	2.3	0.17	411.46	4.21
NoPlant	37	2.3	0.17	417.05	4.12
NoPump	0.1	23.8	0.00	1.43	3.16
SoyPrice	29.1	1.5	0.11	328.22	3.28

5. Conclusions and Recommendations

This study shows that for the chosen example of the Embarras River, the estimated revenue from harvesting a dual-purpose constructed wetland, as proposed in the introduction, is not shown to be sufficient to overcome the costs of building and operating such a wetland. Only in the case where all costs except pumping and piping were ignored was the wetland shown to be profitable. Thus, the operation of a constructed wetland for nutrient removal, even one that produces biofuel stock, will, if this example is typical, continue to be a net-cost proposition.

Still, for the example used here, the task of draining and harvesting the wetland proves to be worthwhile in lowering cost and is thus more efficient than a wetland devoted to water treatment only, at least for smaller wetland sizes. Regardless of wetland size, the difference between a wetland harvested for biomass and a wetland designed exclusively for water quality improvement (in terms of cost efficiency) is minor. Even under an assortment of realistic (and unrealistic) cost scenarios the Pareto frontier showed little variation and yielded a profit only when cost assumptions were dramatically liberal. From a cost efficiency (cost-per-removal) perspective however, there is a small range of wetland areas and pumping capacities that will provide the minimum cost per mass removal of $\text{NO}_3\text{-N}$ for most scenarios examined (except for the NoCapNoOM and NoPump scenarios). In these scenarios, the difference between the values of minimum cost-per-removal was only about a dollar per kilogram of $\text{NO}_3\text{-N}$ removed (values ranged from \$3.28 to \$4.86).

Fortunately, growing interest in agricultural non-point source pollution abatement and biomass production in the Midwest does not completely rule out the future of constructed wetland systems designed for water quality improvement and biomass production. The advent of second generation biofuels has the potential to alter both the physical and economic landscape. The existence of a nitrogen abatement market could be significant in reducing the cost of systems similar to that described above. By earning credits quantified by the amount of $\text{NO}_3\text{-N}$ removed by the wetland, stakeholders in the system would be able to sell these credits to industries, municipalities, and farmers discharging excessive amounts of nitrogen, thus establishing a nitrogen trading market. Besides being a relatively inexpensive way to deal with agricultural nitrate-nitrogen water quality issues, the restoration or creation of wetlands has the potential to provide various benefits such as flood damage reduction and wildlife habitat. Nutrient trading programs for both point and non-point dischargers have been implemented on the watershed scale with varying levels of success throughout the United States. Although the creation of a nitrogen market seems inevitable, cooperation between policy makers and nitrate-nitrogen dischargers (and potentially

nitrogen-abating farmers) will be necessary to assure efficient operation of a nitrogen credit trading system. Current nutrient trading programs rely mostly on the trading of transferrable discharge permits between point dischargers. As compared to non-point source pollution, point-source dischargers are more able closely to monitor their nutrient fluxes. Quantifying the effect of wetlands on water quality proves difficult due to the large influence of variations in natural conditions. If wetlands are to be incorporated into a nutrient trading framework, quantifying the environmental benefits of actual wetland systems will be the major challenge. If a hypothetical wetland were constructed as presented above, in the presence of a nitrogen trading market, one would be able to make design decisions based on the market nitrogen price. To determine exactly how constructed wetlands for biomass harvesting would play into a nitrogen market would require the simulation of a watershed-scale permit trading system involving both non-point and point source agents.

Apart from potential monetary benefits from biomass sales, incorporation of other benefits that wetlands provide into the analysis may make constructed wetlands for biomass production a possibility in the future. Apart from nitrogen removal, wetlands provide environmental benefits in the form of habitat restoration, flood protection, as well as the treatment of other water-borne pollutants. While quantification of such benefits proves difficult, doing so could advocate for the construction of systems as described above.

Although the analysis presented here offers key insights into the behavior of a potential wetland system designed for biomass harvesting and water quality improvement, some recommendations are offered to strengthen and advance the study. First, empirical and pilot studies are necessary not only to validate the simulation and cost models, but to also confirm the feasibility of harvesting biomass as described above. Such a study should be of an experimental wetland in which some hydrophilic biofuel crop is grown and harvested. The empirical data thus generated could be used to improve the calibration of the nutrient removal and biomass production simulation models and could lead to a better understanding of the biomass growth and nutrient removal behavior as a function of temperature, and nutrient concentration. The pilot study would demonstrate the economic feasibility (or lack thereof) of a larger wetland in more nearly full-scale mode for nutrient removal and biofuel production. Besides empirical and pilot studies, analysis of the problem may be enhanced through a more complete integration of the nutrient removal and biomass production model. For example, including a routine that simulates decomposition of accumulated biomass litter into the biomass production model and using the output to adjust denitrification rates in the nutrient removal model could provide further theoretical insight of the effect of harvesting on nutrient removal. A stochastic analysis could also prove useful in further research in order to assess how the

wetland system operates when environmental conditions, such as temperature and streamflow, are not known values as in the deterministic formulation presented above. Such an analysis might even be capable of assessing wetland efficacy in the face of global climate change.

Constructed wetland systems such as the hypothetical one presented in this analysis offer a way to improve water quality while lessening dependence on fossil fuels. Through the cooperation of policy makers and other stakeholders, it is foreseeable that wetland systems designed for nutrient removal and biomass production could provide both environmental and economic benefits.

6. References

- Ailstock, M. S., Norman, C. M., & Bushmann, P. J. (2001). Common reed *phragmites australis*: Control and effects upon biodiversity in freshwater nontidal wetlands. *Restoration Ecology*, 9(1), 49-59.
- Allen, R. G., Pereira, L. S., Raes, D., & Smith, M. (1998). *Crop evapotranspiration-guidelines for computing crop water requirements-FAO irrigation and drainage paper 56*
- Allirand, J., & Gosse, G. (1995). An above-ground biomass production model for a common reed (*phragmites communis trin.*) stand. *Biomass and Bioenergy*, 9(6), 441-448.
- Asaeda, T., & Bon, T. V. (1997). Modelling the effects of macrophytes on algal blooming in eutrophic shallow lakes. *Ecological Modelling*, 104(2-3), 261-287.
- Asaeda, T., & Karunaratne, S. (2000). Dynamic modeling of the growth of *phragmites australis*: Model description. *Aquatic Botany*, 67(4), 301-318.
- Bonham, A. J. (1983). The management of wave-spending vegetation as bank protection against boat wash. *Landscape Planning*, 10(1), 15-30.
- Boyd, C. E. (1970). Amino acid, protein, and caloric content of vascular aquatic macrophytes. *Ecology*, 51(5), 902-906.
- Braskerud, B. C., Tonderski, K. S., Wedding, B., Bakke, R., Blankenberg, A. B., Ulén, B., et al. (2005). Can constructed wetlands reduce the diffuse phosphorus loads to eutrophic water in cold temperate regions? *Journal of Environmental Quality*, 34(6), 2145-2155.
- Brix, H. (1987). Treatment of wastewater in the rhizosphere of wetland plants - the root-zone method. *Water Science and Technology*, 19(1-2), 107-118.
- Cheney, W., & Kincaid, D. (2004). *Numerical methods and computing* (5th ed.). Belmont, CA: Thomson-Brooks/Cole.
- Deb, K., Pratap, A., Agarwal, S., & Meyarivan, T. (2002). A fast and elitist multiobjective genetic algorithm: NSGA-II. *IEEE Transactions on Evolutionary Computation*, 6(2), 182-197.
- Ditomaso, J. M., Reaser, J. K., Dionigi, C. P., Doering, O. C., Chilton, E., Schardt, J. D., et al. (2010). Biofuel vs bioinvasion: Seeding policy priorities. *Environmental Science and Technology*, 44(18), 6906-6910.
- Duffy, M. D., & Nanhou, V. Y. *Costs of producing switchgrass for biomass in Iowa* (2001)
<http://www.extension.iastate.edu/Publications/PM1866.pdf>
- Dykyjova, D., & Pribil, S. (1975). Energy content in the biomass of emergent macrophytes and their ecological efficiency. *Arch. Hydrobiol.*, 75(1), 90-108.
- Engloner, A. I. (2009). Structure, growth dynamics and biomass of reed (*phragmites australis*) - A review. *Flora*, 204(5), 331-346.

- Gersberg, R. M., Elkins, B. V., Lyon, S. R., & Goldman, C. R. (1986). Role of aquatic plants in wastewater treatment by artificial wetlands. *Water Research*, 20(3), 363-368.
- Getsinger, K. D., Nelson, L. S., Glomski, L. A. M., Kafcas, E., Schafer, J., Kogge, S., et al. (2007). *Control of phragmites in a Michigan great lakes marsh-final report-draft*. Vicksburg, MS: U.S. Army Engineer Research and Development Center.
- Granéli, W. (1984). Reed phragmites australis (cav.) trin. ex steudel as an energy source in Sweden. *Biomass*, 4(3), 183-208.
- Hara, T., Van Der Toorn, J., & Mook, J. H. (1993). Growth dynamics and size structure of shoots of phragmites australis, a clonal plant. *Journal of Ecology*, 81(1), 47-60.
- Hargreaves, G. L., Hargreaves, G. H., & Riley, J. P. (1985). Irrigation water requirements for Senegal River basin. *Journal of Irrigation & Drainage Engineering - ASCE*, 111(3), 265-275.
- Haslam, S. M. (1969a). Development and emergence of buds in phragmites communis trin. *Annals of Botany*, 33(130), 289-301.
- Haslam, S. M. (1969b). Development of shoots in phragmites communis trin. *Annals of Botany*, 33(132), 695-709.
- Haslam, S. M. (1970). The development of the annual population in phragmites communis trin. *Annals of Botany*, 34(3), 571-591.
- Hey, D. L. (2002). Nitrogen farming: Harvesting a different crop. *Restoration Ecology*, 10(1), 1-10.
- Hey, D. L., Kenimer, A. L., & Barrett, K. R. (1994). Water quality improvement by four experimental wetlands. *Ecological Engineering*, 3(4), 381-397.
- Ho, Y. B. (1979). Shoot development and production studies of phragmites australis (cav.) trin. ex steudel in scottish lochs. *Hydrobiologia*, 64(3), 215-222.
- Hocking, P. J. (1989a). Seasonal dynamics of production, and nutrient accumulation and cycling by phragmites australis (cav.) trin. ex stuedel in a nutrient-enriched swamp in inland australia. I. whole plants. *Australian Journal of Marine & Freshwater Research*, 40(4), 421-444.
- Hocking, P. J. (1989b). Seasonal dynamics of production, and nutrient accumulation and cycling by phragmites australis (cav.) trin. ex stuedel in a nutrient-enriched swamp in inland australia. II. individual shoots. *Australian Journal of Marine & Freshwater Research*, 40(4), 445-464.
- Hosoi, Y., Kido, Y., Miki, M., & Sumida, M. (1998). Field examination on reed growth, harvest and regeneration for nutrient removal. *Water Science and Technology*, 38(1 pt 1), 351-359.
- House, C. H., Broome, S. W., & Hoover, M. T. (1994). Treatment of nitrogen and phosphorus by a constructed upland-wetland wastewater treatment system. *Water Science and Technology*, 29(4), 177-184.

- Illinois Society of Professional Farm Managers and Rural Appraisers (ISPFMRA). (2006). *2005 Illinois farmland values and lease trends*
- Kadlec, R. H., & Knight, R. L. (1995). *Treatment wetlands*. Boca Raton, FL: CRC Press.
- Kadlec, R. H., & Wallace, S. (2009). *Treatment wetlands* (2nd ed.). Boca Raton, FL: CRC Press.
- Kamio, A. (1985). Studies of the drying of marshy and heavy clay soil ground by means of vegetations: Changes in soil water caused by evapotranspiration by *phragmites communis*. *Journal of Yamagata Agriculture and Forestry Society*, 42, 53-60.
- Kaul, V., & Vass, K. K. (1972). Production studies of some macrophytes of Srinagar lakes. *Proceedings of the IBP-UNESCO Symposium on Productivity Problems of Freshwater*, Kazimierz Dolny, Poland. 6-12.
- Khanna, M., Dhungana, B., & Clifton-Brown, J. (2008). Costs of producing miscanthus and switchgrass for bioenergy in Illinois. *Biomass and Bioenergy*, 32(6), 482-493.
- Kovacic, D. A., David, M. B., Gentry, L. E., Starks, K. M., & Cooke, R. A. (2000). Effectiveness of constructed wetlands in reducing nitrogen and phosphorus export from agricultural tile drainage. *Journal of Environmental Quality*, 29(4), 1262-1274.
- Kovacic, D. A., Twait, R. M., Wallace, M. P., & Bowling, J. M. (2006). Use of created wetlands to improve water quality in the midwest-lake bloomington case study. *Ecological Engineering*, 28(3 SPEC. ISS.), 258-270.
- Kvet, J., Svoboda, J., & Fiala, K. (1969). Canopy development in stands of *typha latifolia* L. and *phragmites communis* Trin. in south moravia. *Hydrobiologia*, 10, 63-75.
- Lake Bloomington Watershed TMDL Implementation Plan* (2008) (Lake Bloomington TMDL). Illinois Environmental Protection Agency. <http://www.epa.state.il.us/water/tmdl/report/bloomington/lake-bloomington.pdf>
- Meuleman, A. F. M., Beekman, J. P., & Verhoeven, J. T. A. (2002). Nutrient retention and nutrient-use efficiency in *phragmites australis* stands after wastewater application. *Wetlands*, 22(4), 712-721.
- NADB database (1998) (NADB v.2). *North American Treatment Wetland Database (NADB), Version 2.0*. Compiled by CH2M Hill, Gainesville, Florida.
- Ng, T. L., & Eheart, J. W. (2008). A multiple-realizations chance-constrained model for optimizing nutrient removal in constructed wetlands. *Water Resources Research*, 44(4)
- Peters, M. S., Timmerhaus, K. D., & West, R. E. (2003). *Plant design and economics for chemical engineers* (5th ed.). New York, NY: McGraw-Hill.
- Released september 11, 2009, by the national agricultural statistics service (NASS), agricultural statistics board, U.* (2009).

- Royer, T. V., David, M. B., & Gentry, L. E. (2006). Timing of riverine export of nitrate and phosphorus from agricultural watersheds in Illinois: Implications for reducing nutrient loading to the Mississippi River. *Environmental Science and Technology*, 40(13), 4126-4131.
- Sakurai, Y., Matsumoto, Y., & Miyairi, M. (1985). Growth rate and productivity of emergent plants in Lake Biwa, Lake Kasumigaura and Chikuma River. *Proceedings of the Annual Meeting of the Japanese Society of Limnology, Kantho-Koshinetsu Branch*, 10 20-21.
- Saltonstall, K. (2002). Cryptic invasion by a non-native genotype of the common reed, *Phragmites australis*, into North America. *Proceedings of the National Academy of Sciences of the United States of America*, 99(4), 2445-2449.
- Scheffer, M., Bakema, A. H., & Wolterboer, F. G. (1993). MEGAPLANT: A simulation model of the dynamics of submerged plants. *Aquatic Botany*, 45(4), 341-356.
- Schnitkey, G. (2003a). Estimated cost of crop production in Illinois. *Farm business management handbook-FBFM 0100*.
http://www.farmdoc.uiuc.edu/manage/enterprise_cost/2003_crop_budgets.pdf
- Schnitkey, G., Lattz, D., & Siemens, J. (2003b). Machinery cost estimates: Field operations. *Farm business management handbook, FBFM 0201*.
http://www.farmdoc.uiuc.edu/manage/pdfs/Mach_field_operations_2003.PDF#
- Sims, R. E. H., Hastings, A., Schlamadinger, B., Taylor, G., & Smith, P. (2006). Energy crops: Current status and future prospects. *Global Change Biology*, 12(11), 2054-2076.
- TMDL development for lake bloomington, illinois this file contains...* (2008).
- Toet, S., Bouwman, M., Cevaai, A., & Verhoeven, J. T. A. (2005). Nutrient removal through autumn harvest of *Phragmites australis* and *Thypha latifolia* shoots in relation to nutrient loading in a wetland system used for polishing sewage treatment plant effluent. *Journal of Environmental Science and Health - Part A Toxic/Hazardous Substances and Environmental Engineering*, 40(6-7), 1133-1156.
- Tré, J., & Lowenberg-Deboer, J. (2005). Ex-ante economic analysis of alternative mulch-based management systems for sustainable plantain production in southeastern Nigeria. *Agricultural Systems*, 86(1), 52-75.
- Turhollow, A. (2000). Costs of producing biomass from riparian buffer strips.
<http://www.oml.gov/~webworks/cpr/v823/rpt/108548.pdf#>
- U.S. Environmental Protection Agency (EPA). (2000). *Constructed wetlands treatment of municipal wastewaters* No. Rep. EPA/635/R-99/010). Cincinnati, OH: Off. of Res. and Devel.
- Waier, P. R. (2006). *Building construction cost data 2006* (64th ed.). Kingston, MA: RS Means.